

T.R.
GEBZE TECHNICAL UNIVERSITY
GRADUATE SCHOOL OF NATURAL AND APPLIED SCIENCES

**EFFECT OF THE HUMAN BONE MARROW STROMAL CELLS
WITH MODIFIED DEK EXPRESSION ON THE MULTIPLE
MYELOMA CELLS**

TÜRKAN GÜZEL
**A THESIS SUBMITTED FOR THE DEGREE OF
DOCTOR OF PHILOSOPHY**
DEPARTMENT OF MOLECULAR BIOLOGY AND GENETICS

GEBZE
2022

T.R.
GEBZE TECHNICAL UNIVERSITY
GRADUATE SCHOOL OF NATURAL AND APPLIED SCIENCES

**EFFECT OF THE HUMAN BONE MARROW
STROMAL CELLS WITH MODIFIED DEK
EXPRESSION ON THE MULTIPLE
MYELOMA CELLS**

TÜRKAN GÜZEL
**A THESIS SUBMITTED FOR THE DEGREE OF
DOCTOR OF PHILOSOPHY**
DEPARTMENT OF MOLECULAR BIOLOGY AND GENETICS

THESIS SUPERVISOR
PROF. DR. AYTEN KANDILCI

GEBZE

2022

**T.C.
GEBZE TEKNİK ÜNİVERSİTESİ
FEN BİLİMLERİ ENSTİTÜSÜ**

**İNSAN KEMİK İLİĞİ STROMA
HÜCRELERİNDEKİ DEK GEN İFADESİ
DEĞİŞİKLİĞİNİN MULTİPLE MİYELOM
HÜCRELERİNE ETKİSİNİN
ARAŞTIRILMASI**

**TÜRKAN GÜZEL
DOKTORA TEZİ
MOLEKÜLER BİYOLOJİ VE GENETİK ANABİLİM DALI**

**DANIŞMANI
PROF. DR. AYTEN KANDİLCİ**

**GEBZE
2022**

GEBZE TEKNİK ÜNİVERSİTESİ

DOKTORA JÜRİ ONAY FORMU

GTÜ Fen Bilimleri Enstitüsü Yönetim Kurulu'nun 07/07/2022 tarih ve 2022/34 sayılı kararıyla oluşturulan jüri tarafından 20/07/2022 tarihinde tez savunma sınavı yapılan Türkan Güzel'in tez çalışması Moleküler Biyoloji ve Genetik Anabilim Dalında DOKTORA tezi olarak kabul edilmiştir.

JÜRİ

ÜYE

(TEZ DANIŞMANI) : Prof. Dr. Ayten KANDİLCİ

ÜYE

: Prof. Dr. Uygur Halis TAZEBAY

ÜYE

: Dr. Öğr. Üyesi Didem ÖZKAN

ÜYE

: Prof. Dr. Nuri ÖZTÜRK

ÜYE

: Prof. Dr. Sema SIRMA EKMEKÇİ

ONAY

Gebze Teknik Üniversitesi Fen Bilimleri Enstitüsü Yönetim Kurulu'nun
...../...../..... tarih ve/..... sayılı kararı.

İMZA/MÜHÜR

SUMMARY

Plasma cells are dependent on bone marrow stromal cells for their differentiation and survival. Bone marrow stromal cells provide a unique microenvironment for normal plasma cells or Multiple myeloma (MM) cells via paracrine factors or cellular interactions. Our previous data showed that certain MM patients have an increased DEK expression level in their bone marrow. Since the DEK overexpression is associated with various cancer types, we suggested that alterations in DEK expression in the tumor microenvironment may contribute to the proliferation or survival of MM cells. Here, we aimed to determine the impact of DEK expression on the bone marrow stromal cells (HS-27A and HS-5) and co-cultured MM cells.

We demonstrated that stable modification of DEK expression moderately slowed proliferation and didn't affect migration of HS-27A cells. In addition, co-culture studies revealed that the proliferation or viability of the MM cells is not affected by DEK modification in stromal cells. However, we detected an association between IL-6 and DEK expression in HS-5 cells for the first time. We also showed that DEK alteration in HS-5 cells slightly affects the secretion of angiogenin (ANG), C-X-C motif chemokine 10 (CXCL10) and YKL-40. Upon these findings, we suggest that modifications of DEK expression in the bone marrow stromal cells may affect the cytokine secretion profile of the cells, which may alter the bone marrow microenvironment.

This project is funded by the Scientific and Technological Research Council of Turkey (TÜBİTAK) Grants (KBAG 212T108 and 118Z664) and Gebze Technical University Research Fund (BAP-2017-A105-40).

Key Words: DEK, Multiple Myeloma, Bone Marrow Stromal Cells, Cytokine, IL-6

ÖZET

Kemik iliği stromal hücreleri, plazma hücrelerinin gelişiminde ve hayatta kalmasında kritik bir rol oynamaktadır. Bu hücreler parakrin faktörler veya hücreler arası etkileşimler yoluyla normal plazma hücreleri veya Multipl miyelom (MM) hücreleri için özel bir mikroçevre sağlarlar. Önceki çalışmalarımız, bazı Multipl Miyelom hastalarının kemik iliğinde DEK ifadesinde artış meydana geldiğini göstermiştir. Aşırı DEK ifadesi çeşitli kanser türleriyle ilişkili olduğundan, tümör mikroçevresinde DEK ekspresyonunda meydana gelen değişikliklerin MM hücrelerinin çoğalmasına veya hayatta kalmasına katkıda bulunabileceği düşünülmüştür. Bu tez çalışmasında, DEK ifadesinin kemik iliği stroma hücrelerinin (HS-27A ve HS-5) ve birlikte kültüre edilen MM hücrelerinin (RPMI-8226 ve U266) biyolojisi üzerindeki etkilerinin belirlenmesi amaçlanmıştır.

Elde edilen bulgular, HS-27A hücrelerinde DEK ifadesinin kalıcı modifikasyonunun hücrelerin proliferasyonunu hafif oranda azalttığını ancak migrasyonunu etkilemediğini göstermiştir. Ayrıca, birlikte kültür çalışmaları sonucunda MM hücrelerinin çoğalmasının veya canlılığının stroma hücrelerindeki DEK modifikasyonundan etkilenmediği belirlenmiştir. Bu tez kapsamında, HS-5 hücrelerinde DEK ve IL-6 ekspresyon seviyesi arasında pozitif bir korelasyon olduğu gösterilmiştir. Ayrıca HS-5 hücrelerindeki DEK değişikliğinin anjiyogenin (ANG), C-X-C motifli kemokin 10 (CXCL10) ve YKL-40 ekspresyon seviyesini hafif oranda etkilediği belirlenmiştir. Elde edilen bulgular, literatürde ilk defa olmak üzere kemik iliği stromal hücrelerindeki DEK ekspresyonu değişikliklerinin hücrelerin sitokin salgı profilini etkileyebileceğini ve sonuç olarak kemik iliği mikroçevresinde değişikliklere yol açabileceğini göstermektedir.

Bu çalışma TÜBİTAK (KBAG 212T108 ve 118Z664) ve Gebze Teknik Üniversitesi BAP (2017-A105-40) tarafından desteklenmiştir.

Anahtar Kelimeler: DEK, Multipl Miyelom, Kemik İliği Mikroçevresi, Sitokin, IL-6

ACKNOWLEDGEMENTS

Initially, I would like to thank my supervisor Prof. Dr. Ayten KANDİLCİ, for providing me this opportunity to do my doctoral studies in her lab. She always shared her valuable knowledge with me at all stages of this thesis study. Thank you for your guidance and support even in my most challenging times.

I am grateful to my committee members for evaluating my dissertation and participating in my PhD defense with helpful remarks and ideas.

My special thanks go to my dear colleague Dr. Z. Onur Çalışkaner for all he did for this and many other projects and for his great friendship. Furthermore, I am grateful to my friends Dr. Merve Tuzlakođlu Öztürk, Sinem Gül, Eda Gazel Pehlivan, Mayıs Gamze Çakırca, Çiđdem Ülküseven Erol, Ömer Güllülü and Abdullah Abdul Waheed. It was always a pleasure to share the same laboratory with you.

I appreciate my dearest friends Elif Teke, Fatma Sađır, Şeyma Özen and Duygu Koca for their sincere friendship.

I am deeply grateful to my beloved husband, Metin Güzel, for his pure love, patience and unconditional support. I appreciate you for always having faith in me and making this journey much easier with your company. I also thank my furry son Askar for choosing me as his human and making my life full of joy.

Finally, my huge thanks go to my dear family, especially my mother, for their unconditional love and support in every period of my life. Thank you for always being by my side.

TABLE of CONTENTS

	<u>Page</u>
SUMMARY	v
ÖZET	vi
ACKNOWLEDGEMENTS	vii
TABLE of CONTENTS	viii
LIST OF ABBREVIATIONS AND ACRONYMS	xi
LIST OF FIGURES	xiv
LIST OF TABLES	xvii
1. INTRODUCTION	1
1.1. The Purpose, Contribution and Content of the Thesis	1
2. HEMATOPOETIC SYSTEM	3
3. B CELLS	5
3.1. B Cell Development	5
3.2. Gene Segment Rearrangements	5
3.3. Elimination of Self-Reactive B Cells	6
3.4. B Cell Activation	6
4. PLASMA CELLS	8
4.1. Plasma Cell Development	8
4.2. Transcription Factors Involved in Plasma Cell Development	8
5. BONE MARROW CELLS	10
6. MULTIPLE MYELOMA	12
6.1. Disease and Symptoms	12
6.2. Development of Multiple Myeloma	12
7. DEK	15
7.1. Structural Properties and Cellular Functions of DEK	15
7.2. DEK and Multiple Myeloma	17
8. MATERIALS	18
9. METHODS	23
9.1. Characteristics of the Cell Lines	23

9.2.1. Bone Marrow Stromal Cell Lines (HS-27A and HS-5)	23
9.2.2. MM Cell Lines (RPMI 8226 and U266)	23
9.2. Maintenance of Cells in the Culture	23
9.3. Splitting and Freezing of Cells	24
9.4. Cell Counts and Calculation of Viability	25
9.5. Modification of DEK Expression in Bone Marrow Stromal Cells	25
9.5.1. Transfection of HEK293T cells	25
9.5.2. Transduction of Bone Marrow Stromal Cells	27
9.5.3. Sorting of GFP ⁺ Cells With FACS	27
9.6. Confirmation of Gene Expression at The RNA Level	28
9.6.1. Total RNA Isolation	28
9.6.2. cDNA Synthesis	28
9.6.3. RT-qPCR	29
9.7. Confirmation of Gene Expression at the Protein Level	31
9.7.1. Protein Isolation	31
9.7.2. BCA Assay	31
9.7.3. SDS Gel Electrophoresis	32
9.7.4. Transfer of Proteins from Gel to Membrane	32
9.7.5. Antibody Application	33
9.7.6. Imaging	33
9.8. WST-1 Assays	34
9.9. Co-Culture of MM Cell Lines with DEK Overexpressing HS-27A Cells	34
9.9.1. Co-Culture with Conditioned Medium (CM)	35
9.9.2. Indirect Co-Culture	36
9.9.3. Direct Co-Culture	36
9.10. Determination of Apoptotic Cell Rate by FACS	36
9.11. Caspase Assay	37
9.12. Wound Healing Assay	37
9.13. TCA Precipitation	37
9.14. Cytokine Array	38
9.15. Statistical Analysis of Data	39
10. RESULTS	40
10.1. Stable Modification of DEK Expression in HS-27A Cells	40
10.2. Confirmation of DEK Expression in HS-27A Cells	41

10.3. Analysis of Proliferation Capacity of DEK Overexpressing HS-27A Cells	43
10.4.1. Co-Culture with Conditioned Medium (CM)	44
10.4.2. Indirect Co-Culture	47
10.4.3. Direct Co-Culture	48
10.5. Determination of Apoptotic Cell Rate in HS-27A Cells after the suppression of DEK expression	49
10.6. Caspase Assay	50
10.7. MCL-1 and p53 Expression in HS-27A Cells Levels	51
10.8. Dilution of Virus Medium for Lentiviral Transduction of HS-27A Cells	52
10.9. WST-1 Proliferation Assay of DEK Downregulated HS-27A Cells	54
10.10. Wound Healing Assay for HS-27A Cells	55
10.11. Modification of DEK Expression in HS-5 Cells	59
10.12. Confirmation of DEK Expression in HS-5 Cells	60
10.13. Determination of IL-6 Expression in HS-5 Cells	61
10.14. Analysis of IL-6 Secretion in the HS-5-shDEK Cells	62
10.15. Cytokine Array	63
11. DISCUSSION	65
REFERENCES	68
BIOGRAPHY	75
APPENDICES	76

LIST OF ABBREVIATIONS AND ACRONYMS

<u>Abbreviations and Acronyms</u>	<u>Explanations</u>
°C	: Degree Celcius
ml	: Milliliter
µl	: Microliter
µm	: Micrometer
kDa	: Kilodalton
7-AAD	: (7-Aminoactinomycin D)
ACTB	: Actin-Beta
AML	: Acute Myeloid Leukemia
ANG	: Angiogenin
BCL6	: B-Cell Lymphoma 6 Protein
BCR	: B Cell Receptor
BLIMP1	: B-Lymphocyte-Induced Maturation Protein 1
BMSCs	: Bone Marrow Stromal Cells
BSA	: Bovine Serum Albumin
cDNA	: Complementary DNA
CLP	: Common Lymphoid Progenitor
CMP	: Common Myeloid Progenitor
CO ₂	: Carbone Dioxide
CSR	: Class Switch Recombination
Ct	: Cycle Treshold
CXCL10	: C-X-C Motif Chemokine Ligand 10
CXCL12	: C-X-C Motif Chemokine Ligand 12
CXCR4	: C-X-C Chemokine Receptor Type 4
dH ₂ O	: Distilled Wated
DMEM	: Dulbecco's Modified Eagle Medium
DMSO	: Dimethyl Sulfoxide
DNA	: Deoxyribonucleic Acid
E2F1	: Transcription Factor E2F1

EDTA	:	Ethylenediaminetetraacetic Acid
FACS	:	Fluorescence Activated Cell Sorting
FBS	:	Fetal Bovine Serum
GAPDH	:	Glyceraldehyde-3-Phosphate Dehydrogenase
GFP	:	Green Fluorescent Protein
GMP	:	Granulocyte and macrophage progenitor
HPRT	:	Hypoxanthine Guanine Phosphoribosyl Transferase
HRP	:	Horseradish Peroxidase
HSC	:	Hematopoietic Stem Cell
Ig	:	Immunoglobulin
IGF-1	:	Insulin-like growth factor 1
IL-10	:	Interleukin-10
IL-6	:	Interleukin-6
IL-7	:	Interleukin-6
MCL1	:	Myeloid Cell Leukemia Sequence 1
MEP	:	Megakaryocyte Erythroid Progenitor
MHC	:	Major Histocompatibility Complex
MM	:	Multiple myeloma
MPPs	:	Multipotent Progenitors
mRNA	:	Messenger Ribonucleic Acid
NF- κ B	:	Nuclear Factor kappa B
NK	:	Natural Killer Cells
PAX5	:	Paired Box Protein 5
PBS	:	Phosphate Buffered Saline
rpm	:	Revolutions Per Minute
RT-qPCR	:	Real Time Polymerase Chain Reaction
SCF	:	Stem Cell Factor
SHM	:	Somatic hypermutation
shRNA	:	Short Hairpin RNA
TBS	:	Tris Buffered Saline
TCA	:	Trichloroacetic acid
VCAM-1	:	Vascular Cell Adhesion Protein 1

VEGF : Vascular endothelial growth factor
VLA-4 : Very Late Antigen 4
WST-1 : Water Soluble Tetrazolium-1
XBP-1 : X-box-binding protein 1



LIST OF FIGURES

<u>Figure No:</u>	<u>Page</u>
2.1: Schematic representation of hematopoiesis.	4
3.1: B cell development and activation.	7
4.2: Transcription factors involved in plasma cell development.	9
5.1: Plasma cell development and survival in the bone marrow.	11
6.1: Development of multiple myeloma.	13
7.1: Structure, regulation and function of DEK protein.	16
9.1: Retroviral MIGR1 plasmid.	26
9.2: Assembly of gel and membrane for transfer cassette.	33
9.3: Approaches for co-culture of MM cells with HS-27A cells.	35
10.1: GFP analysis of HS-27A cells after retroviral transduction.	40
10.2: GFP analysis after lentiviral transduction of HS-27A-sh-Neg (A), HS-27A-shDEK-B (B) and HS-27A-shDEK-C (C) cells.	41
10.3: RT-qPCR analysis of overexpression (A) and downregulation (B) of DEK expression in HS-27A cells.	42
10.4: Western Blotting results for DEK expression in HS-27A cells with DEK overexpression (A) and downregulation (B).	42
10.5: Optimization of proliferation conditions for HS-27A-GFP and HS-27A-DEK-GFP cells.	43
10.6: Growth curves of HS-27A-GFP and HS-27A-DEK-GFP cells.	44
10.7: Optimization of serum amount for growth curves of RPMI-8226 cells cultured with complete (standard) medium (black line), serum-free medium (blue line) or serum-free CM obtained from HS-27A cells (green and red lines for HS-27A-GFP and HS-27A-DEK-GFP, respectively).	45
10.8: Growth curves of RPMI-8226 cells seeded at 5000 cells per well or 30000 cells per well using 50%-CM.	46
10.9: Growth curves of RPMI-8226 (A) and U266 (B) cells seeded at a density of 5×10^3 cells/well using CM obtained from HS-27A-GFP and HS-27A-DEK-GFP cells.	46

10.10: Growth curves of U266 (A) and RPMI-8226 (B) cells co-cultured indirectly with HS-27A-GFP and HS-27A-DEK-GFP cells using hanging inserts.	47
10.11: Annexin-V analysis of RPMI-8226 cells co-cultured indirectly with HS-27A-GFP and HS-27A-DEK-GFP stroma cells using hanging inserts.	48
10.12: Growth curves of U266 (A) and RPMI-8226 (B) cells co-cultured directly with HS-27A-GFP and HS-27A-DEK-GFP stroma cells in the same well.	49
10.13: Annexin V analysis in control (sh-Neg) and shDEK-expressing (shDEK-B and shDEK-C) cells (lef panel) and Annexin-V ⁺ cell ratio (right panel).	50
10.14: Caspase activity in the DEK downregulated HS-27A cells.	51
10.15: Expression levels of MCL-1 (A) and p53 (B) in HS-27A cells with downregulated DEK expression.	52
10.16: GFP analysis after lentiviral transduction of HS-27A cells by diluting virus medium as 1/6 and 1/10.	53
10.17: RT-qPCR analysis for the confirmation of DEK expression at mRNA level after transduction of HS-27A cells by diluting the virus medium at 1/6 and 1/10 ratios.	54
10.18: Growth curves of HS-27A cells seeded as 2,5X10 ³ or 5X10 ³ cells per well.	55
10.22: Images for wounds created using 200 µl and 10µl pipette tips for HS-27A shNeg and HS-27A sh-DEK-B cells at 0h and 24 h (Eclipse Ti-S, Nikon, Magnification 4X).	56
10.23: Wound closure after 0, 12 and 18 hours for HS-27A NI, HS-27A GFP, HS-27A DEK-GFP cells (Eclipse Ti-S, Nikon, Magnification 4X).	57
10.24: Wound closure after 0, 12 and 18 hours for HS-27A NI, HS-27A GFP, HS-27A DEK-GFP cells (Eclipse Ti-S, Nikon, Magnification 4X).	58
10.25: Graphical representation of wound closure rates of HS-27A cells.	58
10.26: GFP analysis of HS-5 cells after FACS sorting of retrovirally transduced cells.	59
10.27: GFP analysis of HS-5-DEK-GFP cells after second FACS sorting.	59
10.28: FACS analysis result after lentiviral transduction of HS-5 cells.	60
10.29: Confirmation of DEK overexpression (A) or downregulation (B and C) in HS-5 cells by RT-qPCR or Western Blotting.	61
10.30: IL-6 expression in HS-5 cells at the mRNA (A) and protein (B) levels.	62

10.31: Detection of secreted IL6 in the medium of HS-5-shDEK-B cells.	63
10.32: Cytokine secretion profile in HS-5 cells altered DEK expression.	64
10.33: Graphical representation of cytokine array results.	65



LIST OF TABLES

<u>Table No:</u>	<u>Page</u>
8.1: Cell lines.	18
8.2: Plasmids.	18
8.3: Taqman primer-probes.	18
8.4: Primer designed.	18
8.5: Antibodies.	19
8.6: Kits.	19
8.7: Chemicals and reagents.	19
8.7: Continue.	21
8.9: Glassware, plastics and consumables.	21
8.10: Equipments.	22
9.1: Components for calcium phosphate transfection of HEK293T with retroviral vectors.	27
9.2: Components for calcium phosphate transfection of HEK293T with lentiviral vectors.	27
9.3: Components for cDNA synthesis.	29
9.4: PCR condition for cDNA synthesis.	29
9.5: Components for RT-qPCR reactions with Taqman Master Mix.	30
9.6: PCR Conditions for RT-qPCR with TaqMan Master Mix.	30
9.7: Components for RT-qPCR reactions with Syber Green Master Mix.	30
9.8: PCR Conditions for RT-qPCR with Syber Green.	30
9.9: RIPA buffer for cell lysis.	31
9.10: Serial dilutions of BSA for BCA.	32
9.11: Antibody dilutions for Western Blotting.	33
10.1: Numerical representation of caspase activity in HS-27A cells with DEK downregulation.	51

1. INTRODUCTION

Plasma cells are responsible for antibody secretion against pathogens, making them one of the most indispensable members of the immune system. They are located in the bone marrow (BM), which provides a unique microenvironment for the plasma cell development [Zhao et al., 2012]. Multiple myeloma (MM) is a malignancy of plasma cells caused by abnormal proliferation of plasma cells in the BM and other extramedullary sites [Yang et al., 2013]. Considering its contributory role in proliferation, survival, and chemoresistance of the MM cells, one foremost strategy ought to be targeting the BM microenvironment. However, despite its prominent role in disease progression, outcomes of paracrine or cellular interactions between the BM microenvironment and the MM cells remain elusive.

DEK oncogene is highly expressed in actively proliferating malignant cells of melanoma, urinary bladder cancer, and retinoblastoma [Carro et al., 2006]. Its upregulation results in proliferation by suppressing cell differentiation, while downregulation of DEK leads to suppression of proliferation by inducing apoptosis [Privette Vinnedge et al., 2011], [Wise-Draper et al., 2009]. In addition, DEK protein functions as an autoantigen in some autoimmune diseases [Tabbert et al., 2006]. Secreted extracellular DEK protein can act as a chemoattractant for immune cells [Mor-Vaknin et al., 2006]. Additionally, neighboring cells can take up extracellular DEK and it can fulfill its intracellular functions in these cells [Saha et al., 2013] Also, it has been reported that changes in DEK expression affect the expression of genes in signaling pathways related to the immune system [Adams et al., 2015].

1.1. The Purpose, Contribution and Content of the Thesis

Our previous findings demonstrated that DEK expression is profoundly decreased in CD138⁺ plasma cells compared to CD138⁻ cells or control bone marrow samples. Gene copy number analysis indicated that DEK copy number is increased in about 10% of MM patients. However, DEK expression is decreased in normal and malignant plasma cells, independent of its gene copy number. Besides, our results indicated that in 12% of MM patients, DEK expression was increased over 2-fold in the BM microenvironment cells [Caliskaner et al., 2017]. Considering the importance

of the BM microenvironment in MM's development, we suggested that alterations of DEK gene expression in the BM stromal cells may change the BM microenvironment and indirectly affect the cellular properties of MM cells.

To test this hypothesis, initially DEK expression in BM stromal cells (HS-27A and HS-5) was stably overexpressed or suppressed using retroviral or lentiviral vectors. Then, modification of DEK expression in BM stromal cells was verified by RT-qPCR and Western Blot analysis. Proliferation and migration capacity of HS-27A cells was examined by WST-1 and wound healing assays. DEK overexpressing HS-27A cells were co-cultured with MM cell lines (RPMI-8226 and U266). WST-1 assay or trypan blue countings were performed to determine proliferation and viability of MM cells. Apoptotic cell rates in MM cells co-cultured with BM stromal cells was analysed by flow cytometry using Annexin-V staining. Expression and secretion of IL-6 in DEK modified HS-5 cells were assessed by Western Blot analysis and TCA precipitation methods, respectively. In addition, cytokine secretion profile of HS-5 cells was examined by cytokine array which provides assessment of 105 cytokines at once.

Although, modification of DEK expression in HS-27A cells moderately slowed the proliferation, it didn't affect migration of the cells. Moreover, co-culture studies revealed that the proliferation, viability, and apoptotic cell ratio of MM cells were not affected by DEK alteration in BM stromal cells. However, we showed that expression and secretion of IL-6 is influenced by DEK in the HS-5 cells. In addition, cytokine array results indicated a slight association between DEK expression and secretion of C-X-C motif chemokine 10 (CXCL10), YKL-40 and angiogenin (ANG), which are essential proteins involved in carcinogenesis or hematopoiesis.

Our findings indicated that modifications of DEK expression in BM stromal cells does not influence the viability or proliferation of MM cells. However, for the first time, it is shown that alteration of DEK expression may affect cytokine expression and secretion profile of the bone marrow stromal cells. Therefore, further studies are needed elucidate the effects of DEK alterations in stromal cells on the cell biology of neighboring cells including MM cells.

2. HEMATOPOETIC SYSTEM

Blood comprises more than ten cell types with various activities such as red blood cells for oxygen or carbondioxide delivery, white blood cells for protection against infections, and platelets for blood coagulation [Rieger and Schroeder, 2012]. Blood is one of the most regenerating tissues since the bone marrow of an adult person generates around one trillion new cells every day [Doulatov et al., 2012]. In this regeneration process, which occurs through a highly complex mechanism called hematopoiesis, while new mature blood cells are produced daily, destruction mechanisms eliminates billions of cells that have completed their life span [Smith, 2003]. Maintaining tissue homeostasis in the hematopoietic system depends on the balance between those production and destruction mechanisms.

A small community of multipotent cells, which are localized in the bone marrow at a rate of 0.01%, have self-renewal ability and can differentiate into all mature blood cells in our body [Nemeth and Bodine, 2007]. Under homeostatic conditions, these multipotent cells, called hematopoietic stem cells (HSCs), remain in the G₀ phase of the cell cycle, unlike short-lived mature blood cells [Seita and Weissman, 2010]. An asymmetric cell division of HSCs leads to the generation of one daughter cell that maintains its stem cell features. In contrast, the other daughter cell differentiates into mature blood cell precursors that lack self-renewal capacity [Nemeth and Bodine, 2007]. Thus, the total stem cell number in the tissue remains constant and new mature blood cells are produced in case of requirement. Errors that occur during the division and differentiation of HSCs may cause some critical consequences for the development of hematopoietic cancers, such as the generation of precursor cells that can self-renew or fail to complete their differentiation [Seita and Weissman, 2010].

Flow cytometry analyses showed that the differentiation capacities of HSCs are decreasing in a hierarchical order [Iwasaki and Akashi, 2007]. Within this hierarchical order, the HSCs which are at the top of this system, primarily constitute multipotent precursor cells that have reduced self-renewal ability and have less differentiation capacity. These cells then differentiate into two separate oligopotent cell lines, common myeloid precursor cells (CMPs) and common lymphoid precursor cells (CLPs), under the control of various factors secreted in the BM microenvironment [Seita and Weissman, 2010]. In the end, myeloid precursor cells give rise to platelets,

erythrocytes, macrophages, granulocytes and megakaryocytes. In contrast, lymphoid precursor cells differentiate into T and B lymphocytes and natural killer (NK) cells. Figure 1 shows the hierarchical structure of hematopoiesis [Reagan and Rosen, 2016].

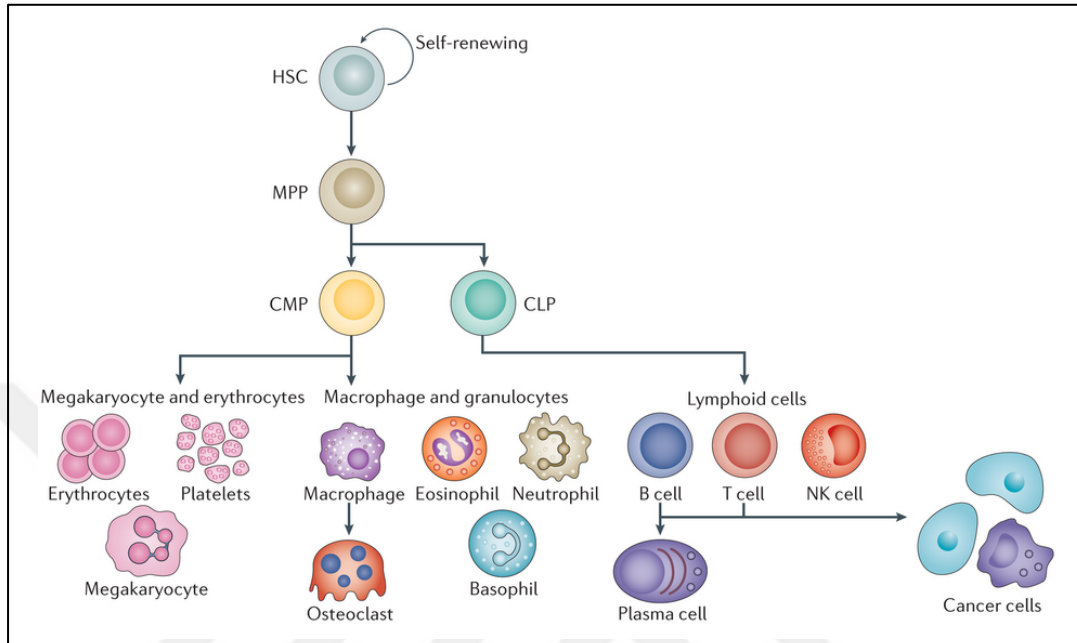


Figure 2.1: Schematic representation of hematopoiesis.

3. B CELLS

3.1. Development of B Cells

B cells are members of the humoral immune system which play role in the body's defense [Maity et al., 2018]. Within the hierarchy of the hematopoietic system, CLPs originating from HSCs differentiate into pro-B cells which have restricted self-renewal capacity. Then, pro-B cells differentiate into pre-B cells and immature B cells, respectively. When immature B cells encounter antigen, B cell differentiation begins in secondary lymphoid tissues [Murphy et al., 2008]. At this stage, gene segment rearrangements occur which lead to high receptor diversity for B cells [Herzog et al., 2009].

3.2. Gene Segment Rearrangements

A large variety of B cells capable of recognizing many antigens are produced in human body. The capacity of B cells to recognize a broad range of antigens is conducted through gene segment rearrangements called V (D)J recombination [Kuehl and Bergsagel, 2002]. During this specific mechanism, the variable (V), diversity-D and joining-J gene regions encoding B cell immunoglobulins are rearranged into different combinations [Herzog et al., 2009]. When B cells undergo V (D)J recombination, D and J segments assemble initially, then the V segments merge with the DJ segments in Ig heavy chain. However, in the Ig light chain, only V and J segments come together [Kuehl and Bergsagel, 2002]. At the end of this process, IgM expressing immature B cells are generated [Tsai et al., 2019].

The V, D and J gene regions are surrounded by recombination signal sequences (RSS). During the rearrangements, RSSs are detected and cleaved by lymphocyte-specific RAG proteins (Recombination activated genes, RAG1 and RAG2) initially. Then, the expression of non-homologous end joining (NHEJ) and DNA repair proteins are stimulated and gene segments are assembled [Schlissel, 2003].

3.3. Elimination of Self-Reactive B Cells

After V(D)J recombination, high diversity of B cell receptors are provided by gene segment rearrangements (Herzog et al., 2009). However, cells that recognize the organism's cells can be generated which may cause autoimmune diseases. Therefore, elimination of these cells by a mechanism called negative selection is crucial to prevent self-reactive cells from harming the body [Burrows et al., 2000]. During negative selection, cells are selected according to their capacity to bind to antigens of the body. Self-reactive cells with strong affinity for self-antigens are clonally deleted via apoptosis. However, cells with low affinity undergo a secondary gene segment rearrangement in their Ig light chain by receptor editing mechanism and escape from clonal deletion if their self-reactivity disappears [Young et al., 2022]. Numerous self-reactive B cells (6-30 %) exit to the periphery but remain silent due to a process called anergy. These cells with low affinity to self antigens are rendered permanently insensitive to antigen by anergy and do not undergo B cell activation when bound to antigen [Cambier et al., 2007].

3.4. Activation of B Cells

After gene segment rearrangements, immature B cells are generated [Pieper et al., 2013]. Then, they detach from the BM and relocate to secondary lymphoid organs. These cells carry IgM on cell surface at this stage [Kuehl and Bergsagel, 2002].

Ig molecules act as B-cell receptors and involved in the activation of the B cells [Maity et al., 2018]. Through these membrane bound receptors, B cells can recognize specific epitopes of many antigens [Murphy et al., 2008]. Upon recognition by the receptor, the antigen is taken into the cell by endocytosis and directed to the lysosomes for degradation. The peptides formed after lysosomal digestion are loaded to particular molecules involved in presentation of antigens called major histocompatibility complex II (MHC II). Then, MHC II-antigen complex is translocated on cell surface and antigen is presented to T cells [Avalos and Ploegh, 2014]. T cells previously activated with the same antigen recognize the MHC II-antigen complex on the B cell surface and secrete cytokines necessary for B cell activation like IL-4 or IL-6 [Murphy et al., 2008]. Upon the activation, B cells begins to proliferate and germinal centers

are generated in the lymph nodes. Then cells differentiate into memory B cells or plasma cells secreting different immunoglobulins such as IgG, IgA, IgE or IgD [Kuehl and Bergsagel, 2002]. Figure 3.1 shows development and activation of B cells [Kuehl and Bergsagel, 2002].

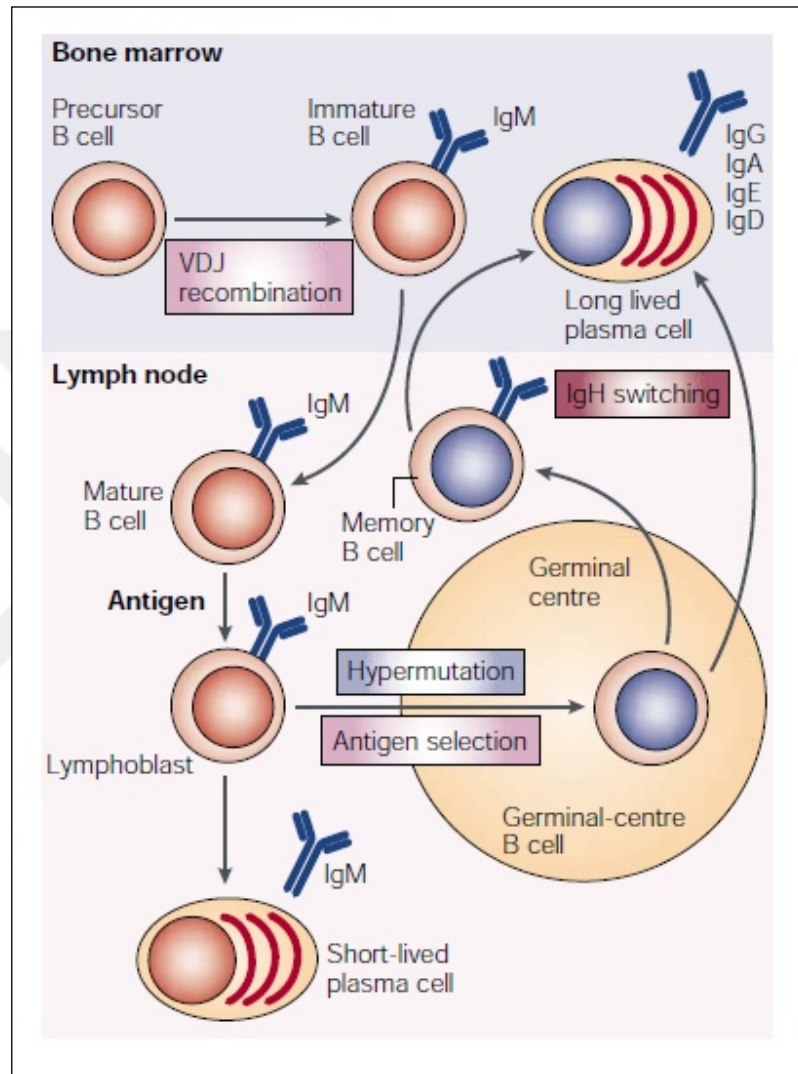


Figure 3.1: B cell development and activation.

4. PLASMA CELLS

4.1. Development of Plasma Cells

Plasma cells are differentiated B cells that secrete antibodies. [D'Souza and Bhattacharya, 2019]. Their percentage is lower than 1% in human lymphoid organs [Fairfax et al., 2008]. Upon to activation by antigen, mature B cells differentiate into centroblasts and start to proliferate clonally [Kuehl and Bergsagel, 2002]. Proliferating centroblasts form germinal centers in secondary lymphoid tissues. Further proliferation of these cells lead to formation of dark zone in the germinal center [Klein and Dalla-Favera, 2008]. In the germinal center, the variable regions of Ig light and heavy chains of cells undergo mutations by a mechanism called somatic hypermutation, thus improving the affinity of antibodies to the antigen [Goossens et al., 1998], [Shapiro-Shelef and Calame, 2005]. The centroblast cells then differentiate into centrocytes which then undergo selection for their antigen affinity with the help of antigen-presenting cells. Cells with high affinity undergo immunoglobulin class switching so that they can secrete other Ig types (IgG, IgA, IgE and IgD) in addition to IgM. Durig the selection, centrocytes with low affinity are eliminated by apoptosis. [Klein and Dalla-Favera, 2008]. Thus, centrocytes differentiate into plasmablasts and then into plasma cells or memory B cells and located to the bone marrow [Klein and Dalla-Favera, 2008], [Kuehl and Bergsagel, 2002].

4.2. Transcriptional Control of Plasma Cell Development

Differentiation of plasma cells is controlled strictly by several transcription factors. BLIMP1 is the most critical gene that stimulates differentiation of plasma cells [Turner et al., 1994]. It represses transcription factors including c-Myc and E2F-1 and trigger cell cycle arrest. Therefore, it inhibits B cell proliferation and stimulates differentiation [Shapiro-Shelef and Calame, 2005]. Additionally, BLIMP-1 triggers the expression of genes related to antibody secretion [Shapiro-Shelef and Calame, 2005]. Moreover, BLIMP-1 suppresses the expression of cell cycle related genes [Shaffer et al., 2002]. It represses transcription factor E2F and regulates the expression of the DEK [Carro et al., 2006]. X box-binding protein 1 (XBP-1) is another crucial

protein involved in plasma cell development [Pieper et al., 2013]. In a plasma cell, very high amount of proteins are synthesized to provide constant antibody production. BLIMP-1 effectively triggers unfolded protein response (UPR) for the proper folding of proteins. This effect is achieved by stimulating the expression of XBP-1 and other genes involved in the UPR [Lee et al., 2003].

Plasma cell development is under the control of additional factors. PAX5 is ensures the maintenance of B cell character by triggering differentiation of CLPs into B cells [Pieper et al., 2013]. BCL6 play role in formation of germinal center and suppresses B cell differentiation. Thus, PAX5 and BCL6 together suppress plasma cell differentiation while maintaining B cell character [Fairfax et al., 2008].

The balance between stimulation (by BLIMP1 and XBP1) and suppression (by PAX5 and BCL6) of differentiation is schematized in Figure 4.2 [Shapiro-Shelef and Calame, 2005].

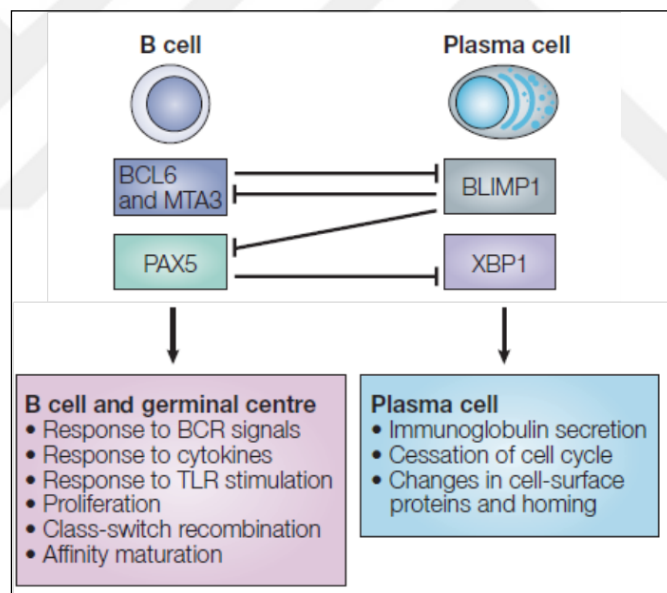


Figure 4.2: Transcriptional control of plasma cell development.

5. BONE MARROW CELLS

Hematopoiesis occurs in the bone marrow which is considered as one of the primary lymphoid organs. There are many cells such as BM stromal cells, osteoblasts, adipocytes and hematopoietic cells [Anthony and Link, 2014].

These cells, particularly stroma cells, create a unique microenvironment for B cells and other hematopoietic cells in the BM. Interactions between B cells and stromal cells, which are driven by adhesion molecules, are crucial during B cell development. In addition, growth factors and cytokines secreted by stromal cells control B cell development and maturation. For example, stem cell factor (SCF), which is bound by c-Kit on mature B cells, and IL-7, which is involved in the development and growth of late pre-B cells, are among the important cytokines secreted by stromal cells [Murphy et al., 2008]. CXCL12 chemokine secreted by stromal cells is a chemokine essential for B cell development and binds to the CXCR4 receptor on B cells. In addition, CXCL12 secreted by stroma cells causes multipotent progenitor cells to migrate towards stroma cells and triggers the release of IL7, which is vital for development of B cells [Tokoyoda et al., 2004].

Additionally, the localization and survival of B cell-derived plasma cells in the BM microenvironment is also controlled by cellular interactions mediated by various cytokines such as IL-6 and cell adhesion proteins such as very late antigen-4 (VLA-4) expressed by BM stromal cells. Furthermore, the differentiation of plasmablasts into memory B cells is also triggered by CXCL12 secreted by stromal cells [Zhao et al., 2012].

Studies indicated that BM stromal cells in the microenvironment, are involved in the development of MM [Mahindra et al., 2010]. IL-6 expression triggers proliferation through STAT3 activation in MM cells and leads to chemotherapeutic drug resistance by suppressing apoptosis through antiapoptotic Bcl-2 family proteins [Derenne et al., 2002]. In addition, pathways including MAPK and PI3K/AKT, which are effective in cell survival, are stimulated by IL-6 in MM [Hideshima et al., 2001]. Moreover, it has been shown that IL-6 increases angiogenesis in the BM by increasing expression of VEGF and enabling the infiltration of MM cells [Dankbar et al., 2000].

Additionally, it has been determined that the accumulation of MM cells in the BM leads to the proliferation of stromal cells due to the changes in the BM

microenvironment [Mahindra et al., 2010], [Noll et al., 2014]. Figure 5.1. shows the factors involved in plasma cell development and survival in the BM [Shapiro-Shelef and Calame, 2005].

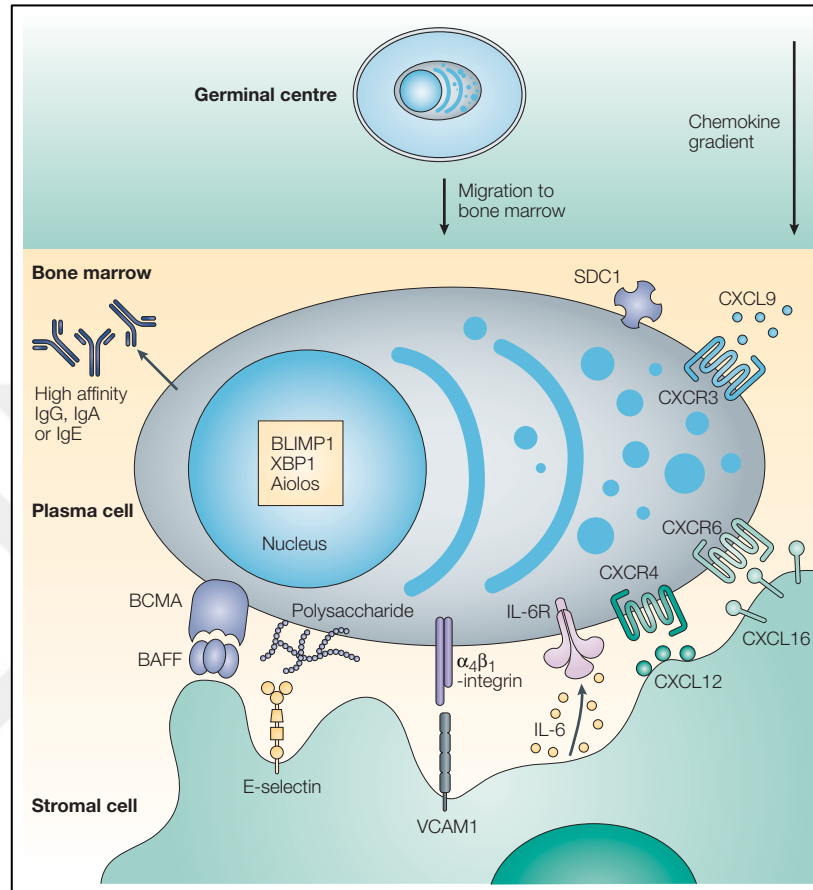


Figure 5.1: Plasma cell development and survival in the bone marrow.

6. MULTIPLE MYELOMA

6.1. Disease and Symptoms

MM is a hematologic cancer type that caused by the abnormal plasma cell expansion and accumulation in the BM [Slovak, 2011]. MM constitute 2% of all cancers and almost 20% of hematologic cancers in USA [Kuehl and Bergsagel, 2002]. Males have a higher prevalence of MM than females, and the average age of onset is 65 years [Kyle et al., 2003]. Current treatment methods aim to regress the disease and prolong survival time, but there is no definitive treatment for MM [Yang et al., 2013].

The presence of 10% or more plasma cells in the BM is the main criterion for the characterization of the disease [Rajkumar et al., 2014]. Detection of monoclonal protein (M protein) or immunoglobulin light chain in serum or urine is another important criteria for diagnosis of MM [Chesi and Bergsagel, 2013]. Additional symptoms are anemia, bone lesions, renal failure, immunodeficiency and hypercalcemia (increased blood calcium levels) [Singhal and Mehta, 2006]. MM cells invade the bone structure cytokines are secreted by malignant plasma cells. Because of many cytokines osteoclast activity is increased and leads to destruction of the bone matrix. Lesions in the bone structure cause a 20% increase in pathologic bone fractures because of the disruption of the balance between osteoclast and osteoblast cells. Bone fractures and osteoporosis cause bone pain for the patients. In addition, increased osteoclast activity results in hypercalcemia [Galson et al., 2012]. Renal failure resulting from immunoglobulin light chain accumulation is observed in 80% of cases [Korbet and Schwartz, 2006].

6.2. Development of Multiple Myeloma

MM results from clonal expansion of plasma cells in the germinal centers of secondary lymphoid organs. Genetic and microenvironmental factors act in the development and progression of the MM. The course of the disease usually starts with Monoclonal Gammopathy of Unknown Significance (MGUS) and ends with the transformation of MGUS to Smoldering Myeloma and then to MM [Kuehl and

Bergsagel, 2002]. Figure 6.1. shows the development of Multiple Myeloma [Kumar et al., 2017].

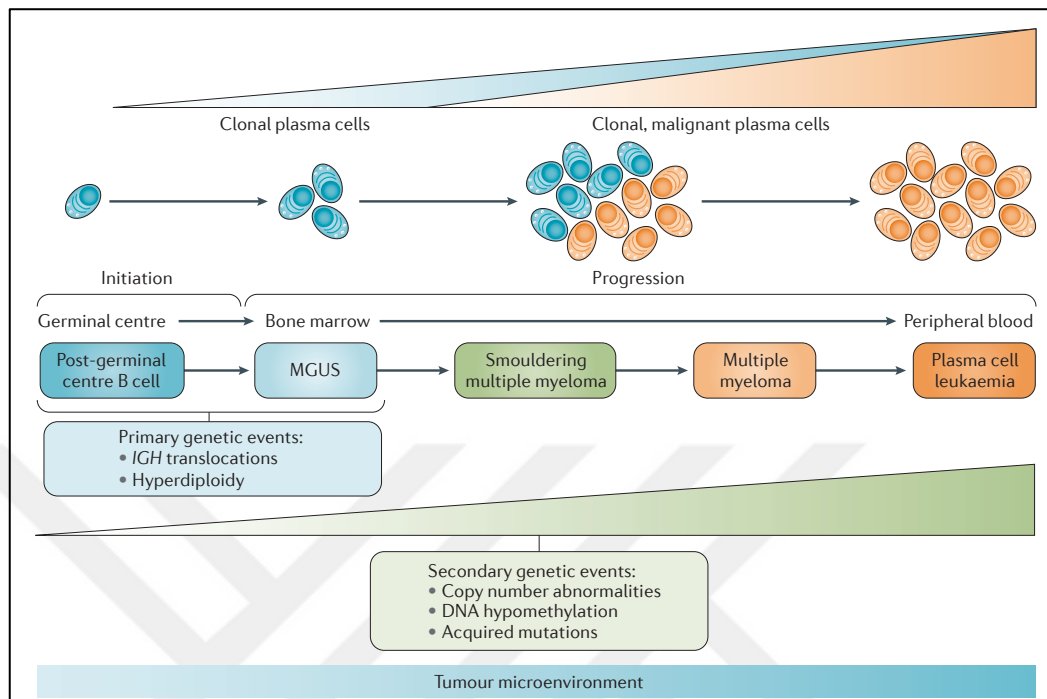


Figure 6.1: Development of multiple myeloma.

Many genetic abnormalities are observed in MM cells [Avet-Loiseau et al., 2007]. MM cells have many complex genetic abnormalities that results from mutations occur during normal development of B cells, such as VDJ recombinations, somatic hypermutations and immunoglobulin alterations [Avet-Loiseau et al., 2007], [Sirohi and Powles, 2004]. Chromosomal translocations between Ig gene segments with strong promoters and oncogenes during VDJ recombinations lead to increased expression of the relevant oncogenes [Bergsagel et al., 1996], [Gonzalez et al., 2007]. Additionally, point mutations in numerous genes, including MYC, NRAS, KRAS, FGFR3 and TP53 [Raab et al., 2009] and chromosomal deletions in the regions of tumor suppressor genes, including retinoblastoma1 and p53 [Fonseca et al., 2009], [Pichiorri et al., 2010] have been reported in MM. Moreover, increases in gene copy number have been detected in MM [Walker et al., 2010]. These genetic alterations are frequently observed in MM patients and accompany a poor prognosis.

Depending on the risk factors and complications, different treatment strategies including chemo-radiotherapy and autologous stem cell transplantation (SCT) are

primarily used in the treatment of MM. Prednisone and chemo-radiotherapy are used in following treatment to prevent relapse. The use of immunomodulatory agents like thalidomide and proteasome inhibitors like bortezomib has increased the survival time of MM patients [Falco et al., 2007], [Kumar et al., 2008]. For MM patients who are suitable for SCT, primary recommended treatment is the combination of bortezomib/cyclophosphamide/ dexamethasone. On the other hand, bortezomib/dexamethasone or melphalan/ prednisone/ lenalidomide treatment is suggested for patients who are not suitable for SCT. The disease relapses in the most of the cases [Yang et al., 2013]. Thus, it is essential to elucidate the molecular mechanisms important for the progression of the MM and to develop more effective treatment strategies.



7. DEK

7.1. Structural Properties and Cellular Functions of DEK

The DEK was characterized in fusion with the NUP214 (CAN) protein as a result of the t(6;9) translocation in an acute myeloid leukemia (AML) patient [von Lindern et al., 1992]. *DEK* gene, which is evolutionarily conserved in many organisms, is localized in the chromosome 6p22.3 in humans and encodes the 43 kDa DEK protein containing 375 amino acids [Carro et al., 2006], [Oancea et al., 2010]. The human DEK protein contains one DNA binding site and 4 acidic sites. It binds to the DNA by its SAP domain and is involved in chromatin organization [Kappes et al., 2004].

DEK which is a nuclear oncoprotein, is highly expressed in numerous of cell types [Kappes et al., 2001]. It takes places in many cellular mechanisms, including DNA repair and replication, transcriptional regulation and maintenance of chromatin structure. Copy number increases particularly in the 6p22.3 chromosome region and transcription factors such as estrogen receptor- α (E α), E2F and NF-Y are associated with the overexpression of DEK [Yu et al., 2016]. Figure 7.1. shows the structure, regulation and function of DEK [Riveiro-Falkenbach and Soengas, 2010].

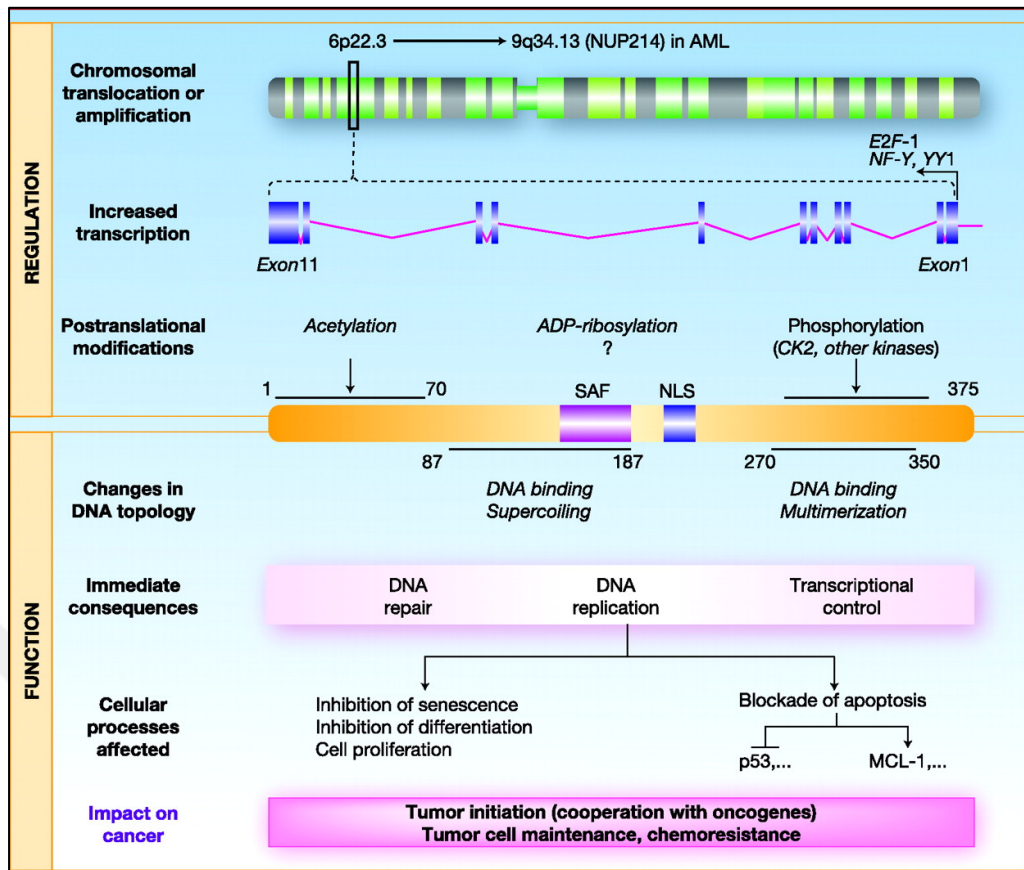


Figure 7.1: Structure, regulation and function of DEK protein.

DEK expression is elevated in lots of cancer types such as hepatocellular carcinoma [Kondoh et al., 1999], retinoblastoma [Grasemann et al., 2005], melanoma [Khodadoust et al., 2009] and bladder cancer [Evans et al., 2004]. DEK acts as a proto-oncogene by suppressing apoptosis and senescence. In addition, it affects cellular proliferation, contributes to metastasis and chemoresistance of cancer cells [Logan et al., 2015]. DEK overexpression results in increased cell proliferation by suppressing differentiation in keratinocytes and breast cancer cells. However, its suppression triggers differentiation and suppresses the proliferation of the cells [Privette Vinnedge et al., 2011], [Wise-Draper et al., 2009]. Suppression of DEK expression in HeLa cells, initiates apoptosis by stabilizing p53 protein [Wise-Draper et al., 2006]. In melanoma cells with suppressed DEK expression, apoptosis occurs through MCL-1, an anti-apoptotic protein independent of p53 protein [Khodadoust et al., 2009].

It has been revealed that DEK knockout mice have higher numbers of hematopoietic progenitor cells and enhanced capacity for colony formation. These data imply that DEK reduces the amount of HPCs by controlling their proliferation

[Broxmeyer et al., 2012]. Furthermore, DEK function as an autoantigen in several autoimmune diseases. It is secreted to extracellular spaces and act as a chemoattractant for neutrophils and cytotoxic T cells [Mor-Vaknin et al., 2006], [Waldmann et al., 2004]. Secreted DEK can be relocalized to the cell nucleus by neighboring cells via endocytosis and fulfills its actions in DNA repair mechanisms or reverses the chromatin damage due to DEK suppression [Saha et al., 2013].

7.2. DEK and Multiple Myeloma

Chromosome 6p is among the regions with an increased copy number in MM. It was shown that 22.8% of MM cases had an increased copy number in chromosome 6 in CD138⁺ plasma cells from MM patients. The region with the highest copy number increase was 6p22.3, where the DEK gene is also localized [Walker et al., 2010]. Our previous finding revealed that DEK expression is downregulated in CD138⁺ MM cells compared to CD138⁻ cells in the BM, independent of the *DEK* gene copy number. Moreover, RT-qPCR results indicated that 12% of MM patients have over a 2-fold increase in DEK expression in the BM microenvironment cells [Caliskaner et al., 2017]. Considering the significance of the BM microenvironment in MM's development and drug resistance, we suggested that alterations of DEK gene expression in the BM stromal cells may change the BM microenvironment and indirectly affect the cellular properties of MM cells.

8. MATERIALS

Table 8.1: Cell lines.

Name	Catalogue Number	Company
HS-27A	-	Dr. Gerard Grosveld
HS-5	-	Dr. Özden Yalçın Özuysal
RPMI 8226	CCL-155	ATCC
U266	TIB-196	ATCC
HEK 293T	-	Dr. Gerard Grosveld

Table 8.2: Plasmids.

Name	Catalogue Number	Company
DEK Human shRNA Plasmid Kit	TL313507	Origene
MIGR1 Retroviral vectors	27490	Addgene
Packaging vectors	-	Dr. Gerard Grosveld

Table 8.3: Taqman primer-probes.

Name	Catalogue Number	Company
DEK	Hs00180127_m1	Applied Biosystems
ACTB	Hs01060665_g1	Applied Biosystems

Table 8.4: Primer designed.

Name	Sequences (5'-3')	Company
IL6 Forward	CCCCAGTACCCCCAGG AGAAGA	MedSanTek
IL6 Reverse	GCTGCGCAGAATGAGA TGAGTTGT	MedSanTek
MCL-1 Forward	ATGCTTCGGAAACTGG ACAT	İontek
MCL-1 Reverse	TCCTGATGCCACCTTCT AGG	İontek
HPRT Forward	GGCAGTATAATCCAAA GATGGTCAA	İontek
HPRT Reverse	GTCTGGCTTATATCCAA CACTTCGT	İontek

Table 8.5: Antibodies.

Name	Catalogue Number	Company
Mouse anti-Human DEK antibody	610948	BD
Mouse anti-Human IL-6	MAB206	R&D systems
Rabbit anti-Human GAPDH antibody	5174P	Cell Signaling
Mouse IgG1 Isotype control Antibody	MAB002	R&D
Mouse anti-Human p53 Antibody	2524	CST
HRP- conjugated anti-rabbit IgG Secondary Antibody	7074P2	Cell Signaling
HRP-conjugated anti-Mouse IgG Secondary Antibody	7076S	Cell Signaling

Table 8.6: Kits.

Name	Catalogue Number	Company
Pierce BCA Protein Assay	23227	Thermo Scientific
ProFection® Mammalian Transfection System	E1200	Promega
High Capacity cDNA Reverse Transcription Kit	4368814	Applied Biosystems
Caspase Colorimetric Sampler Kit	KHZ1001	Thermo Scientific
Human XL Cytokine Array Kit	ARY022B	R&D Systems

Table 8.7: Chemicals and reagents.

Name	Catalogue Number	Company
RPMI Medium	22400-089	Gibco
DMEM	41966029	Gibco
Penicilin/Streptomycin	151401	Gibco
FBS	26140-111	Gibco
DPBS	14190094	Gibco
Trypsin 0.05% EDTA	25300054	Gibco
DMSO	BP231-1	Fisher Scientific
Tryphan Blue	T10282	Invitrogen
Polybrene	H-9268	Sigma-Aldrich
WST-1 Proliferation Reagent	5015944001	Roche

Table 8.7: Continue.

Name	Catalogue Number	Company
Staurosporine	S5921	Sigma-Aldrich
Tripure Isolation Reagent	11667157001	Roche
Isopropanol	24137-2.5L-R	Sigma-Aldrich
Chloroform	24216-2.5L-R	Sigma-Aldrich
2X Taqman Universal Master	4324018	Applied Biosystems
Power Syber Green Master Mix	4367659	Applied Biosystems
Nuclease Free Water	AM9932	Ambion
RNase	2272G4	Ambion
Absolute Ethanol	32221	Sigma-Aldrich
HEPES	H4034-25G	Sigma-Aldrich
Sodium Chloride	S7653-250G	Sigma-Aldrich
Sodium Deoxycholate	D6750-10G	Sigma-Aldrich
Trizma Base Reagent	T1503-1KG	Sigma-Aldrich
SDS	L3771-100G	Sigma-Aldrich
NaCl	S7653-250G	Sigma-Aldrich
NP-40	A1694,0250	Applichem
Tween20	P9416-50ML	Sigma-Aldrich
Protease/Phosphatase Inhibitor Coctail	78440	Thermo Scientific
EDTA	BP118-500	Fisher Chemical
4X Laemmli SDS Buffer	161-0747	Biorad
Beta-mercaptoethanol	A1108.0100	Applichem
BSA	A2153-10G	Sigma-Aldrich
Skim Milk Powder	AB0830,0500	Applichem
Protein Ladder	26616	Thermo Scientific
TBS	TBS999	ScyTek Laboratories
SDS Running Buffer	161-0732	Biorad
10x Tris/Glycine Transfer Buffer	1610734	Biorad
Pierce™ ECL Plus Western Blotting Substrate	32132	Thermo Scientific
Methanol	34885-2.5L-R	Sigma-Aldrich
Acetone	W332615	Sigma-Aldrich
TCA	T0699	Sigma-Aldrich

Table 8.7: Continue.

Name	Catalogue Number	Company
APC Annexin V	550474	BD Biosciences
Formalin	15552	Sigma Aldrich
Crystal Violet	1.014.080.100	Merck
7-AAD Viability Staining Solution	420403	Biolegend

Table 8.9: Glassware, plastics and consumables.

Name	Catalogue Number	Company
T25 Flasks	90026 90076	TPP
T75 Flasks	90076	TPP
Petri Dishes (100×20 mm)	93100	TPP
6 Well Plates	92006	TPP
15 ml Falcon Tubes	91015	TPP
50 ml Falcon Tubes	91050	TPP
Millicell Hanging Cell Culture Inserts	PIHT30R48	Millipore
Thoma Counting Chambers	I.075.03.002	Isolab
Countess™ Cell Counting Chamber Slides	C10228	Invitrogen
Cryo Tubes	89012	TPP
Freezing Container	5100-0001	Nalgene
0.45 mm Syringe Filters	4614	Life Sciences
0.22 mm Syringe Filters	99722	TPP
Cell Strainers (40µm)	352340	BD
Polystyrene Tubes	352063	BD
Qpcr 96 Well Plates	321-75-051	Axygen
Clear Adhesive Film	4306311	Applied
Pcr Tubes	PCR-02-C	Axygen
Eppendorf Tubes	MCT-060-C / 150-C	Axygen
10 µl Filter Tips	BT10XL	Axygen
20 µl Filter Tips	BT20	Axygen
200 µl Filter Tips	BT200	Axygen
1000 µl Filter Tips	BT1250	Axygen
Parafilm	058.01.001	Isolab

Table 8.9: Continue.

Name	Catalogue Number	Company
Trans-Blot Turbo Midi 0.2 μ m Nitrocellulose Transfer Packs	170-4159	Biorad
Any kD™ Mini-PROTEAN® TGX™ Precast Protein Gels	456-9033	Biorad

Table 8.10: Equipments.

Name	Catalogue Number	Company
Cell Culture Hood	Puricube 1200	Cryste
CO2 Incubator	HF90	Heal Force
Water Bath	0400702135J036	Wisd Lab. Ins.
Countess Cell Counter	1754B	Invitrogen
Liquid Nitrogen Tank	LS4800	Taylor Wharton
Inverted Light Microscope	Eclipse TS100	Nikon
Inverted Fluorescence Microscope	Eclipse 80i	Nikon
Light Microscope	Eclipse, E100	Nikon
Flow Cytometer	Accuri C6 Plus	BD
FACS Jazz Cell Sorter	655487	BD
qPCR	Stratagene	Agilent
Thermal Cycler	MJ-Mini PTC1148	Bio-Rad
Nanodrop	206-26300-48	Shimadzu Biotech
Shaker	S2025-B-230V	Labnet
Rotater	Multi RS-60	Biosan
Varioskan Plate Reader	3001-1571	Thermo Scientific
Transblot Tranfer System	170-4155	Biorad
Chemi Doc XRS+	721BR04545	Biorad
Pipetman Starter Kit	F167300	Gilson
Centrifuge	1-14	Sigma
Vortex	444-1372	VWR International

9. METHODS

9.1. Characteristics of the Cell Lines

9.2.1. BM Stromal Cell Lines (HS-27A and HS-5)

HS-27A and HS-5 cells are immortalized healthy human BM cells that grow adherently and have fibroblast cell morphology. BM stromal cells obtained from a 30-year-old healthy individual are transformed using pLXSN16E6E7 plasmid, which contains the gene region encoding the E6 and E7 proteins produced by human papillomavirus. After immortalizing cells, 27 clones were isolated and numbered from 1 to 27 [Web 1, 2022].

Among these clones, HS-5 cells originating from clone number five were found to sustain the proliferation of hematopoietic precursor cells without any additional factor in serum-free medium conditions. HS-5 cells secrete high amounts of cytokines, including IL-6 and IL-8 [Web 2, 2022].

HS-27A is a subclone derived from clone 27. HS-27A cells express high amounts of vascular cell adhesion molecule 1 (VCAM-1) and establish many intercellular interactions with neighboring cells with the large polygonal structures they form [Web 1, 2022], [Web 2, 2022].

9.2.2. MM Cell Lines (RPMI 8226 and U266)

RPMI 8226 and U266 cell lines, the most frequently used cells in MM studies, grow in suspension. U266 cells were obtained by isolating B cells from a 53-year-old MM patient and secrete high amounts of IL6 [Web 3, 2022]. RPMI 8226 cells were obtained from a 61-year-old plasmacytoma patient [Web 4, 2022].

9.2. Maintenance of Cells in the Culture

Human BM stromal cell lines (HS-27A and HS-5) were cultivated in RPMI 1640 medium containing 10% (v/v) FBS and 1% (v/v) penicillin/streptomycin according to the culture conditions recommended by ATCC. MM cell lines (U266 and RPMI 8226)

were cultivated in RPMI 1640 medium containing 15% (v/v) FBS and 1% (v/v) penicillin/streptomycin due to their higher serum requirements. We used HEK 293T cells for virus production. These cells are frequently preferred as packaging cells in viral transduction processes because of their production of high viral titers. For the culture of 293T cells, DMEM medium containing high glucose including 10% (v/v) FBS and 1% (v/v) penicillin/streptomycin was used. All cells were cultivated at 37°C in a humidified incubator with 5% CO₂.

9.3. Splitting and Freezing of Cells

Adherent cells were splitted when confluency reached about 70-80%. First, the old medium was discarded completely and cells were washed with 5 ml of PBS. For enzymatic elimination of cell-cell and cell-surface junctions, 1ml 1X Trypsin-EDTA was added, and cells were incubated at 37°C for 2-3 min. In order to stop the enzymatic activity of trypsin, 8 ml of fresh medium containing serum was added and cells were collected in the falcon tubes. After centrifugation (1000 rpm, 5 min), pellets were resuspended with the appropriate amount of fresh medium, and cells were seeded into new flasks (5×10^5 cells per T25 flasks for HS-5 and HS-27A).

For suspension cell lines, cells were collected to the falcon tubes by centrifugation (5 min, 1000 rpm). The old medium was removed and pellets were dissolved with the appropriate amount of fresh medium. Cells were seeded into new flasks (2×10^6 cells per T25 flasks for U266 and RPMI 8226) and subcultured every 2-3 days when the medium color changed to yellow.

To freeze the cells, the respective amounts were collected to the falcon tubes ($\sim 3 \times 10^6$ viable cells for HS-27A, HS-5 and HEK 293T cell lines, $\sim 6 \times 10^6$ viable cells for U266 and RPMI 8226 cell lines). Supernatants were removed after centrifugation and pellets were resuspended with 1ml freezing medium (90% (v/v) FBS and 10% (v/v) DMSO). Cells were transferred to cryotubes and kept at -80°C for one day in a freezing container with isopropanol for gradual cooling. Then, cryotubes were removed to a liquid nitrogen tank for long-term storage.

9.4. Cell Countings and Calculation of Viability

To calculate the number of the cells, cells and trypan blue were mixed with a ratio of 1:1 and then 10 μ l of samples were loaded to a thoma counting chamber. Cells were counted under the microscope and viability was calculated as percentage. Live cells with intact cell membranes stay colorless because trypan blue does not diffuse into the cell, while dead cells take dye into the cell because of disrupted membrane integrity. Therefore, the live cells appear bright, while the dead cells are observed as blue under the microscope [Crowley et al., 2016].

9.5. Modification of DEK Expression in Bone Marrow Stromal Cells

9.5.1. Transfection of HEK293T cells

HEK 293T cells were seeded ($3,5 \times 10^6$ cells per 10 cm petri dishes) and transfection was performed the next day when cells reached 60-70% confluency. Three to four hours before the transfection, the old medium was removed and fresh DMEM medium containing 10% (v/v) FBS (heat-inactivated for 1 hour at 55°) and 1% (v/v) pen/strep was added to the cells.

For stable overexpression of DEK, retroviral MSCV-DEK-IRES-GFP plasmid was used (Figure 9.1) [Web 5, 2022]. IRES (Internal Ribosomal Entry Site) in the plasmid allowed independent expression of DEK and green fluorescent protein (GFP) under the control of the MSCV (murine stem cell virus) promoter. MSCV-IRES-GFP plasmid was used as a negative control for retroviral transductions. For stable knockdown of DEK, cells were transduced with lentiviral pGFP-C-shLenti vectors. DEK mRNA was targeted by two different 29-mer shRNA constructs (shDEK-B and shDEK-C) in a lentiviral GFP vector. A non-targeting 29-mer scrambled shRNA (sh-Neg) was utilized as a negative control. GFP was reporter gene to identify transduced cells for retroviral and lentiviral vectors.

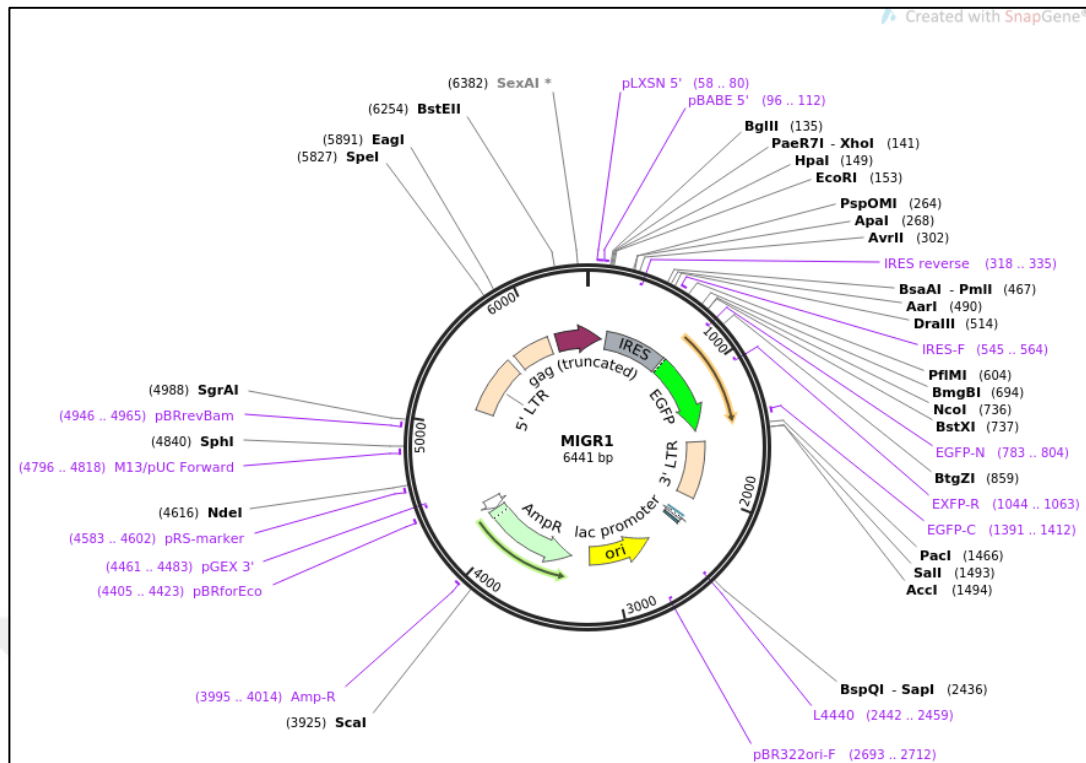


Figure 9.1: Retroviral MIGR1 plasmid.

Transfections were performed using components indicated in Tables 9.1 and 9.2 for retroviral and lentiviral vectors, respectively. As recommended by the manufacturer (Promega calcium phosphate transfection kit), one tube with plasmids, CaCl_2 and dH_2O was prepared and DNA- CaCl_2 solution was added dropwise to a polystyrene tube containing 500 μl of 2X HBS under the mild vortexing. Then, the solution was incubated at room temperature (RT) for 20 minutes and distributed slowly and evenly to the medium of the cells. The medium was removed after 18 hours and 5ml fresh medium was added to each petri dish following the washing cells twice with PBS. After 24 hours, cells were examined under the microscope and GFP^+ cells were accepted as transfected cells. Upon the evaluation of transfection efficiency by microscopy, the virus-containing medium was harvested from the petri dishes, filtered using a sterile 0.45 μm filter and used for infection of BM stromal cell lines.

Table 9.1: Components for calcium phosphate transfection of HEK293T with retroviral vectors.

Component	Stock	Volume
DEK or GFP plasmids (MSCV-DEK-IRES-GFP or MSCV-IRES-GFP)	1 µg/ µl	10 µl
Gag-Pol (Packaging vector)	2 µg/µl	2 µl
VSV-G (Packaging vector)	1 µg/µl	2 µl
Calcium Chloride	2,5 M	50 µl
2X HBS	-	500 µl
Sterile Water	-	436 µl
Total		1000 µl

Table 9.2: Components for calcium phosphate transfection of HEK293T with lentiviral vectors.

Component	Stock	Volume
sh-RNA (shDEK-B, shDEK-C or sh-Neg)	1 µg/µl	10
Gp1R (Packaging vector)	3 µg/µl	2
RTR2 (Packaging vector)	1 µg/µl	2
VsVG (Packaging vector)	1 µg/µl	2
Calcium Chloride	2,5 M	50 µl
2X HBS	-	500 µl
Sterile Water	-	434 µl
Total		1000ul

9.5.2. Transduction of BM Stromal Cells

HS-5 or HS-27A cells were seeded in T25 flasks (5×10^5 cells per flask) 24 hours prior to transduction. The old medium was discarded completely and 3 ml of virus-containing medium with 8µg/ml polybrene was added to the cells. Next day, the old virus-containing medium was discarded, cells were washed, 5 ml fresh medium was added to the cells. Transduction was confirmed by monitoring GFP⁺ cells under the inverted fluorescence microscope.

9.5.3. Sorting of GFP⁺ Cells With FACS

After transduction, GFP⁺ cells were sorted using FACS. Approximately 10×10^6 cells were collected by centrifugation and pellet was resuspended in 10 ml cell sorting

medium (PBS containing 2% BSA and 4 mM EDTA). Cells were filtered using a 40- μ m filter to remove clumps just before sorting. During sorting, GFP⁺ cells were harvested into a falcon tube containing 1 ml of chilled RPMI 1640 medium with 50% FBS. After sorting, GFP⁺ cell ratio was analyzed to check the purity of the cells. After, centrifugation (10 minutes, 1000 rpm), cells were propagated in culture for further experiments.

9.6. Confirmation of Gene Expression at The RNA Level

9.6.1. Total RNA Isolation

Approximately $1,5 \times 10^6$ cells were harvested by centrifugation (4°C, 10 minutes, 1000 rpm). Cell pellets were washed with 6 ml cold PBS and the pellets were resuspended with 1 ml Tripure Isolation Reagent well by pipetting. Then 200 μ l chloroform was added to the samples and incubated for about 3 minutes at RT. Samples were centrifuged (4°C, 15 minutes, 14000 rpm) and a 3-phase solution was obtained. The RNA containing uppermost phase was transferred to fresh eppendorf and 500 μ l of 100% isopropanol was added to the samples. After incubation at RT for 10 minutes, samples were centrifuged (14000 rpm, 10 minutes, 4°C). Next, pellets were washed 2 times with 75% ethanol and centrifuged (4°C, 5 minutes, 14000 rpm). Pelletes (RNA) were air-dried at RT, then dissolved with 40 μ l of RNase-free water. RNA concentrations were measured by nanodrop machine and samples were immediately stored at -80°C.

9.6.2. cDNA Synthesis

High Capacity cDNA Reverse Transcriptase Kit was utilized for cDNA synthesis. Following the method recommended in the kit, a master mix was prepared on ice using the components listed in Table 9.3. Master mix was distributed as 10 μ l to the PCR tubes and for each sample 10 μ l RNA samples (500ng) were added separately. Then, cDNA synthesis was performed using the run method explained in Table 9.4 in a total volume of 20 μ l.

Table 9.3: Components for cDNA synthesis.

Component	Volume
10X RT Buffer	2 μ l
10X RT Random Primers	2 μ l
dNTP Mix (100 mM)	0,8 μ l
Reverse Transcriptase (50 U/ μ l)	1 μ l
RNase Inhibitor (20 U/ μ l)	1 μ l
Nuclease-free Water	3,2 μ l
RNA (50 ng/ μ l)	10 μ l (added separately)
Total	20 μl

Table 9.4: PCR condition for cDNA synthesis.

Temperature	Duration
25°C	10 min
37°C	2 hours
85°C	5 minutes
4°C	∞

9.6.3. RT-qPCR

RT-qPCR was used to analyse the gene expression. Syber Green master mix was utilized for *IL6*, *MCL-1* and *HPRT* and Taqman master mix was used for *DEK* and *ACTB*. Master mixes were prepared on ice using components listed in Table 9.5 or Table 9.6 for Taqman and Syber Green master mixes, respectively. Master mix was distributed to 96 well plates and cDNA samples were added separately for each sample. Then, RT-qPCR was conducted in a volume of 20 μ l using the PCR condition explained in Table 9.7 or Table 9.8.

Ct (threshold cycle) values were obtained separately for each gene after RT-qPCR reaction. Δ Ct value was calculated for each sample by subtracting Ct value for a gene from the Ct value of the reference gene (housekeeping genes *ACTB* or *HPRT* were used as reference genes) of the same sample. Then, the Δ Ct value of each sample was subtracted from the Δ Ct value of the control sample (uninfected cell or negative control cells), so that the $\Delta\Delta$ Ct value was obtained. Using formula $2^{-[\Delta\Delta Ct]}$, the change in gene expression was calculated as fold change, indicating the decrease or increase of the expression level for the gene of interest compared to the control sample.

Table 9.5: Components for RT-qPCR reactions with Taqman Master Mix.

Component	Volume
2X Taqman Gene Expression Master Mix	10 μ l
Taqman Gene Expression Assay (<i>DEK</i> or <i>ACTB</i>)	1 μ l
Nuclease-free Water	7 μ l
cDNA	2 μ l (added separately)
Total	20 μl

Table 9.6: PCR Conditions for RT-qPCR with TaqMan Master Mix.

Temperature	Duration	Cycle Number
50°C	2 minutes	1
95°C	10 minutes	1
95°C	15 seconds	40
60°C	1 minutes	

Table 9.7: Components for RT-qPCR reactions with Syber Green Master Mix.

Component	Volume
Power Syber Green Master Mix	10 μ l
Forward Primer	0,6 μ l
Forward Primer	0,6 μ l
Nuclease-free Water	7,2 μ l
cDNA	1 μ l
Total	20 μl

Table 9.8: PCR Conditions for RT-qPCR with Syber Green.

Temperature	Duration	Cycle Number
95°C	3 minutes	1
95°C	30 sec	40
55°C	30 seconds	
72°C	1 minutes	
72°C	10 minutes	1

9.7. Confirmation of Gene Expression at the Protein Level

9.7.1. Protein Isolation

Approximately 3×10^6 cells were collected by centrifugation (4°C, 10 minutes, 1000 rpm). Next, the pellets were washed with cold PBS and centrifuged (4°C, 10 minutes, 1500 rpm). For lysis, 100 µl RIPA buffer was added to the pellets and mixed well. Samples were incubated on ice for 30 minutes and centrifuged (13000 rpm, 10 minutes, 4°C). Finally, the supernatant was transferred to the new eppendorfs and samples were stored at -80°C.

Table 9.9: RIPA buffer for cell lysis.

Component	Final Concentration
Sodium Chloride	150 mM
Sodium Deoxycolate	%0,5 (v/v)
Tris-HCl (pH=8.0)	50 mM
SDS	%0,1 (v/v)
NP40	%1 (v/v)
Protease Phosphatase Inhibitor (100X)	1X (added freshly)

9.7.2. BCA Assay

Protein concentration was evaluated using Pierce BCA Protein Assay Kit following the method recommended by the company. Briefly, the working solution was prepared by mixing solution A and solution B with a ratio of 50:1. Next, 200 µl of the working solution was added to each well in a 96-well plate. Standards of known concentrations were prepared by serial dilution of bovine serum albumin protein as indicated in Table 9.10. Then, 25 µl of samples or standards were added to the wells in duplicate. The plate was incubated on a shaker at 37°C for 30 min in the dark. After 5 minutes of cooling, absorbance values for each well were measured at 562 nm using the plate reader. The absorbance values were averaged and a standard curve graph was generated using the values of standard samples. Finally, the protein concentration was determined for each sample using the formula acquired from the graph.

Table 9.10: Serial dilutions of BSA for BCA.

Sample	Volume of Diluent	Volume of BSA	Final Concentration (µg/ml)
A (Stock)	-	300 µl of A	2000
B	125 µl	375 µl of A	1500
C	325 µl	325 µl of A	1000
D	175 µl	175 µl of B	750
E	325 µl	325 µl of C	500
F	325 µl	325 µl of E	250
G	325 µl	325 µl of F	125
H	400 µl	100 µl of G	25
I (Blank)	400 µl	-	0

9.7.3. SDS Gel Electrophoresis

A denaturing 10% mini protean ready-to-use gel was used for SDS gel electrophoresis. The gel was placed in the vertical electrophoresis system and the tank was sufficiently filled with running buffer (1X). Based on the BCA results, the volume for 30 µg protein samples was mixed with 4X loading buffer containing 10% beta-mercaptoethanol. The final volume was adjusted to 20 µl with dH₂O for each sample. Samples were boiled at 95°C for 5 minutes and then loaded into the gel after removing of the comb. The gel was run at 80 Volt for about 10 minutes and then at 100 Volt for approximately 2 hours.

9.7.4. Transfer of Proteins from Gel to Membrane

Ready-to-use nitrocellulose transfer packs were used for transfer of proteins. The transfer cassette was prepared as shown in Figure 9.2. A blotting roller was used to remove air bubbles and some 1X transfer buffer was poured over the sandwich to prevent drying-out (Web 6, 2022). Then, the sandwich was placed in the transblot device and transfer was performed at 2,5 A and 25 Volt for 7 minutes.

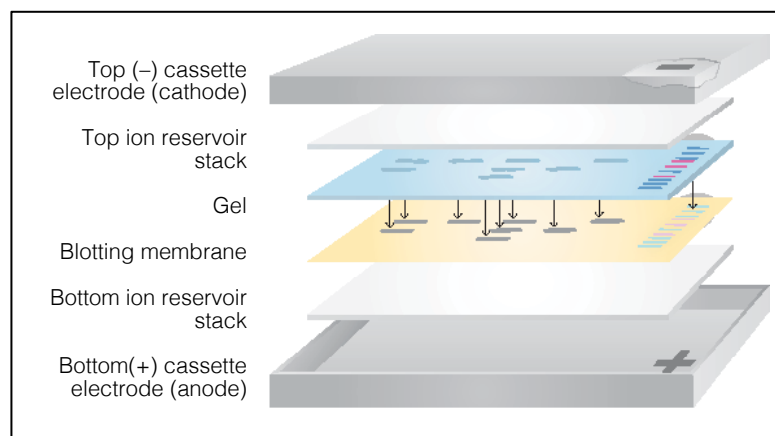


Figure 9.2: Assembly of gel and membrane for transfer cassette.

9.7.5. Antibody Application

The membrane washed with TBS-T (1X TBS solution containing 0.1% Tween-20) for approximately 1-2 minutes and then it was blocked for 1 hour with 5% BSA solution by rotating at RT. Next, it was incubated with a primary antibody prepared with 5% BSA solution at 4°C overnight on a rotator (Dilutions and incubation times for each antibody are listed in the Table 9.11). Then, the membrane was washed 3 times with TBS-T solution for 10 minutes at RT and secondary antibodies (anti-Mouse or anti-Rabbit) were applied 1 hour at RT, rotating. Finally, the membrane was washed with TBS-T solution 3 times and prepared for chemiluminescent imaging.

Table 9.11: Antibody dilutions for Western Blotting.

Antibody	Dilution	Duration	Temperature
Mouse anti-human DEK	2:1000	Overnight	4°C
Mouse anti-human IL-6	1 µg/ml	Overnight	4°C
Rabbit anti-human GAPDH	1:5000	Overnight	4°C
HRP-conjugated anti-mouse	3:10000	1 hour	RT
HRP-conjugated anti-rabbit	1:3000	1 hour	RT

9.7.6. Imaging

For imaging, 1ml of substrate working solution was prepared by combining solution A and solution B at a 40:1 ratio. Then, the membrane was placed in the Chemi

Doc XRS+ imaging system, working solution was distributed dropwise over the membrane to cover the entire area, and images were taken using Image Lab. 4.0.1 program.

9.8. WST-1 Assays

WST-1 assay was performed to determine the proliferation and viability of the cells. WST-1, which is stable a tetrazolium salt, is reduced to a soluble formazan dye because of mitochondrial dehydrogenase enzyme activity in living cells. This reduction cause a color change and measurements of the absorbance directly reflect the number of viable cells [Scarcello et al., 2020].

HS-27A or MM cells were seeded in 96-well plates as triplicates with 200 μ l volume and cell-free RPMI 1640 medium was used as blank. Then, proliferation was monitored for five consecutive days. A relevant plate was taken every day and 20 μ l of WST-1 dye was added to each well. Then, the plate was incubated at 37°C in a 5% CO₂ incubator for 4 hours and absorbance values were measured at 455 nm using a plate reader. Blank values were subtracted from each sample and a growth curve was generated.

9.9. Co-Culture of MM Cell Lines with DEK Overexpressing HS-27A Cells

For co-culture experiments, three different approaches were followed as shown in Figure 9.3:

- Co-culture with Conditioned Medium (CM): CM obtained from HS-27A cells were used to culture MM cells. Therefore, only the effects of paracrine factors (cytokines, growth factors, etc.) secreted by stromal cells on MM cells were investigated.
- Indirect Co-Culture: HS-27A cells and MM cells were cultured in the same well without direct cell-to-cell interactions so that reciprocal effects of paracrine factors (cytokines, growth factors, etc.) secreted from stromal cells and MM cells were examined.

- Direct Co-Culture: HS-27A cells and MM cells were cultured in the same well directly. Thus, the effects of direct cell-to-cell interactions by adhesion molecules, paracrine or autocrine factors (cytokines, chemokines, growth factors, etc.) were analyzed.

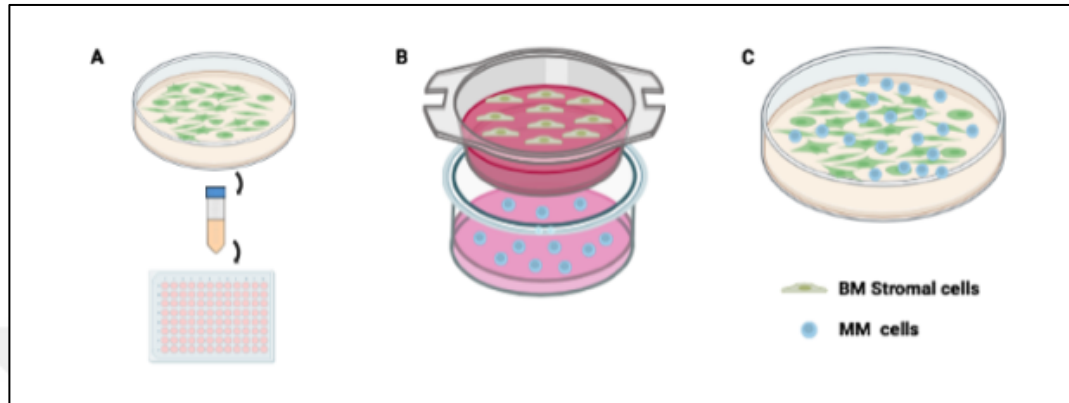


Figure 9.3: Approaches for co-culture of MM cells with HS-27A cells. (A) Co-culture with CM, (B) indirect co-culture, (C) direct co-culture.

9.9.1. Co-Culture with Conditioned Medium (CM)

HS-27A-GFP and HS-27A-DEK-GFP cells were used to obtain conditioned medium (CM) and MM cell lines were cultured with this medium. To prepare CM, control HS-27A cells were seeded into T75 flasks (1.5×10^6 cells per flask) and cultivated for three days until cells reached the confluency. The old medium was removed and cells were washed with PBS. Fifteen ml of serum-free RPMI 1640 medium was added to the cells. After 18 hours, serum-free medium on cells, the so-called conditioned medium (CM), was collected and passed through a sterile $0.22 \mu\text{m}$ filter to eliminate dead or live cells.

First, to compare the proliferation of RPMI-8226 cells with or without serum conditions, cells were cultured using complete medium (containing 15% serum), serum-free medium or serum-free CM. The RPMI-8226 cells were seeded in a 96-well plate (30000 cells/well) as triplicates in 200 μl volume. Cell-free medium was used as blank for each experimental group, and proliferation was monitored in 96-well plates for 5 days by using WST-1 assay as described before.

Afterwards, 50%-CM was obtained by adding fresh RPMI 1640 medium containing 15% serum at a ratio of 1:1 to the CM obtained from HS-27A cells. Then,

RPMI-8226 cells were seeded (5000 or 30000 cells/well) using the 50% CM to optimize the cell density. Next, WST-1 was used and growth curves were generated for five days. Further experiments were performed with the selected cell density.

9.9.2. Indirect Co-Culture

For indirect co-culture studies, HS-27A cells and MM cells were cultured in the same well without direct cell-to-cell contact by placing a special hanging insert. Hanging inserts allow fluidic flow between cells but prevent cell migration due to their 0,4 μm pores. Briefly, HS-27A cells were seeded as replicates with a density of 2×10^5 cells per hanging insert and MM cells (RPMI-8226 or U266) were seeded as 6×10^5 cells/well in 6-well plates. Then, individual hanging inserts with HS-27A cells were placed in 6-well plates with MM cells. At 48h and 96h, inserts were removed from the respective plates and cell proliferation was determined for MM cells. The growth curves of U266 cells were obtained by taking 100 μl of the cell mixture on the relevant days and applying WST-1 as described before. RPMI-8226 cells were counted by trypan blue staining or Annexin-V/FACS analysis was conducted to evaluate apoptotic cell rates.

9.9.3. Direct Co-Culture

HS-27A cells were co-cultured with MM cells in the same well without inserts to observe the impacts of direct cell-to-cell interactions, adhesion molecules and paracrine factors. HS-27A cells were seeded (5×10^3 cells/well) as triplicates in 96-well plates and U266 cells were seeded to the same wells (3×10^4 cells/well). Proliferation was monitored for 5 days using WST-1. Additionally, HS-27A cells and RPMI 8226 cells were seeded as 2×10^5 and 6×10^5 cells/well in 6-well plates as replicates. Then, cells were counted by using trypan blue staining.

9.10. Determination of Apoptotic Cell Rate by FACS

Approximately 3×10^5 cells were collected by centrifugation (1000 rpm, 10 min). After washing with chilled PBS, the pellet was dissolved in 100 μl 1X Annexin Binding Buffer. 5 μl APC Annexin V was added to the cells, vortexed briefly and

incubated for 15 min in the dark at RT. Then, cells were resuspended with 300 μ l of 1X Annexin Binding Buffer, briefly vortexed and analyzed using BD Accuri.

9.11. Caspase Assay

Caspase protein activity (caspase 2, 3, 6, 8 and 9) in HS-27A cells was detected using Caspase Colorimetric Sampler Kit. HS-27A cells treated with 0,25 μ M Staurosporine for 16 hours were used as a positive control. Following the kit's instructions, approximately 20×10^6 cells were harvested by centrifugation (1000 rpm, 10 min). The pellet was dissolved in 200 μ l of lysis buffer, incubated on ice for 10 min and centrifuged (1 min, 10000 g). The supernatant was transferred to new tubes and protein quantification was performed. 50 μ l of protein sample (175 μ g) was loaded into each well of a 96-well plate and 50 μ l of 2X Reaction buffer containing 10 mM DTT was added. Then, 5 μ l of substrate for each caspase protein were added to the wells. Samples were incubated in the dark at 37°C for 2 hours and absorbance values were measured at 400 nm using a plate reader.

9.12. Wound Healing Assay

HS-27A cells were seeded (2×10^5 cells/well) in 6-well plates using complete medium (containing 10% FBS). After four days, when they reached 100% confluency, a wound-like cell-free space was created by drawing a line along the cell surface using 10 μ l or 200 μ l pipette tips. Cell-free space was examined for 24 hours under the inverted microscope. The appropriate time units and pipette tip was decided by analyzing the closure rates of the wounds. Then, the experiments were performed three times the indicated time conditions. Images were analyzed with ImageJ (ImageJ 1.52a) software.

9.13. TCA Precipitation

HS-5 cells were seeded (1×10^6 cells) in T25 flasks and cultured for two days to let them reach the confluency. Then, the old medium was removed and cells were washed with PBS. Serum-free RPMI 1640 medium was added to the cells and after

two days of culture, serum-free medium was collected. Next, TCA precipitation was performed to detect proteins secreted in the medium. Medium and TCA were mixed in a ratio of 1:4 and incubated for 10 minutes at 4°C. Samples were centrifuged (14000 rpm, 5 minutes, 4°C). Then, the supernatant was removed and the pellet was washed with chilled acetone twice. After centrifugation, the supernatant was discarded completely and the pellet was dried at 95°C for 5 minutes. Finally, pellet was dissolved by using the 4X Laemli buffer and samples were loaded to the SDS page gel for Western Blotting.

9.14. Cytokine Array

A cytokine array was used to determine the changes in cytokine secretion of HS-5 cells due upon modification of endogenous DEK expression. 1×10^6 cells were seeded in T25 flasks and cultured for 48 hours to let them reach the confluency. Then, the old medium was discarded and 2 ml serum-free RPMI 1640 medium was added to the flasks. After 48 hours, the serum-free medium was collected and cytokine array was performed following the method recommended by the manufacturer (Human XL Cytokine Array Kit). First, 4 membranes provided by the kit were blocked separately with 2 mL of array-buffer-6 for 1 hour on a shaker, in the 4-Well Multi-dish. Then, the serum-free medium was diluted by mixing 500 μ l medium with array-buffer-6 and final volume was adjusted to 1.5 mL. After blocking buffer was discarded and diluted samples were added to the membranes. Next, membranes were incubated overnight on a shaker at 4°C and washed 3 times with 1X wash buffer. Afterwards, 30 μ L of Detection Antibody Cocktail was diluted with 1.5 mL of 1X Array Buffer 4/6 and added to the membranes. After 1 hour of incubation, membranes were washed 3 times with 1X Wash Buffer. Next, membranes were placed into the 4-Well Multi-dish and 2 mL of 1X Streptavidin-HRP was added to each well. Then, they were incubated for 30 minutes at RT on a shaker. After the washing steps, excess wash buffer was removed. Membranes were placed onto a plastic sheet and 1 ml of the Chemi Reagent Mix was distributed onto membranes. Next, membranes were carefully covered with the top sheet of plastic and after removing the air bubbles, they were incubated for 1 minute. Excess Chemi Reagent Mix was removed by blotting paper towels to the edge of the membranes and images were taken using Chemi Doc XRS+ imaging system.

9.15. Statistical Analysis of Data

GraphPad Prism 6 software was used to conduct statistical analyses. The statistical significance of the data obtained from independent experiments was assessed by two way ANOVA multiple comparison tests based on the experimental design, such as the number of replicates and groups. P values $<0,05$ were accepted as significant.



10. RESULTS

10.1. Stable Modification of DEK Expression in HS-27A Cells

Initially, we generated HS-27A cells that either overexpress DEK or suppress endogenous DEK expression. First, DEK was stably overexpressed in HS-27A cells by retroviral vectors. Upon transduction, GFP analysis was carried out by flow cytometry. Results showed that transduction efficiency was 72% and 29% for HS-27A-GFP (control cells) and HS-27A-DEK-GFP cells, respectively. Cells were sorted by FACS and GFP⁺ cell ratios were increased to 84% and 90% for control and HS-27A-DEK-GFP cells, respectively (Figure 10.1). Cells were considered pure enough to be used in further studies.

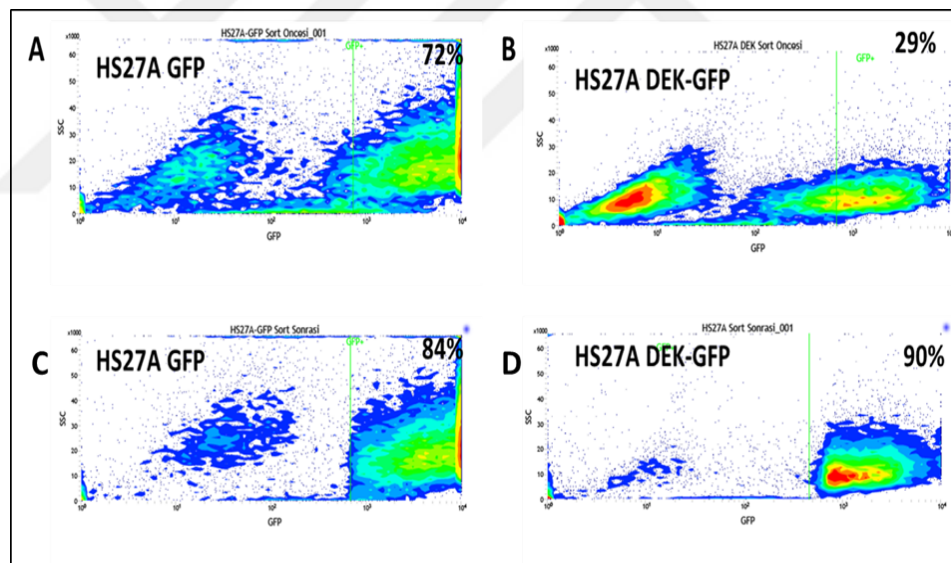


Figure 10.1: GFP analysis of HS-27A cells after retroviral transduction. A and C showing GFP analysis results of control HS-27A-GFP cells before and after sorting, respectively. B and D showing GFP analysis results of HS-27A-DEK-GFP cells before and after sorting, respectively.

Secondly, DEK expression was downregulated in HS-27A cells using two different DEK targeting shRNAs (shDEK-B and shDEK-C). A scrambled non-targeting shNeg vector was used as a negative control. Flow cytometry analysis showed that GFP⁺ cell ratios were 82,5%, 91,5% and 85% for HS-27A-sh-Neg (control

cells targeted by a non-human gene specific sh-RNA), HS-27A-shDEK-B and HS-27A-shDEK-C cells, respectively (Figure 2). Due to the already high GFP⁺ cell ratios, cells were used as such in the following experiments.

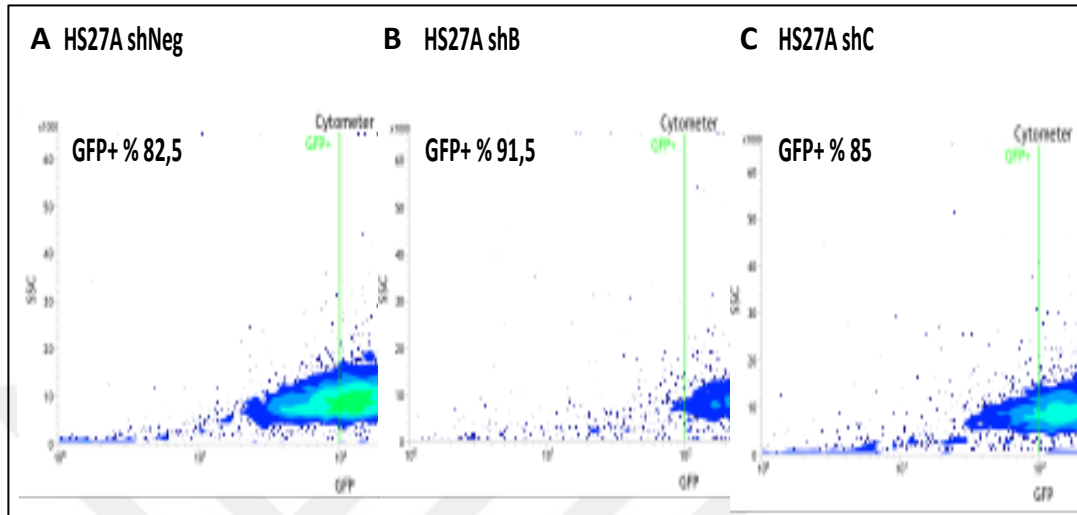


Figure 10.2: GFP analysis after lentiviral transduction of HS-27A-sh-Neg (A), HS-27A-shDEK-B (B) and HS-27A-shDEK-C (C) cells.

10.2. Confirmation of DEK Expression in HS-27A Cells

RT-qPCR analysis was performed to confirm DEK expression at the mRNA level. To do this, sorted GFP⁺ HS-27A cells were used for RNA isolations. RT-qPCR results indicated that DEK expression was increased approximately 14-fold in HS-27A-DEK-GFP cells compared to control cells (Figure 10.3A). Conversely, DEK expression was decreased by 84% and 20% in HS-27A-sh-DEK-B and HS-27A-sh-DEK-C cells, respectively, compared to HS-27A-shNeg cells (Figure 10.3B).

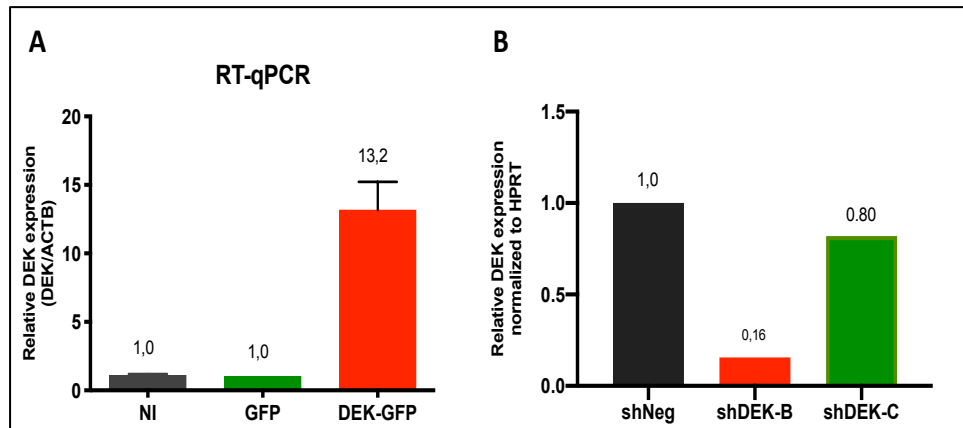


Figure 10.3: RT-qPCR analysis of overexpression (A) and downregulation (B) of DEK expression in HS-27A cells. NI: Uninfected parental HS-27A cells.

Afterwards, DEK expression in HS-27A cells was determined at the protein level using an anti-DEK antibody. Western Blotting results showed that the DEK band belonging to HS-27A-DEK-GFP cells was more robust than the band belonging to control HS-27A-GFP cells, confirming DEK overexpression (Figure 10.4A). On the other hand, as expected DEK expression was suppressed in the HS-27A-sh-DEK-B and sh-DEK-C cells and they exhibited weaker DEK bands compared to the control cells (Figure 10.4B). GAPDH was used as a loading control. DEK protein levels in HS-27A cells were similar to the relative mRNA levels calculated by RT-qPCR.

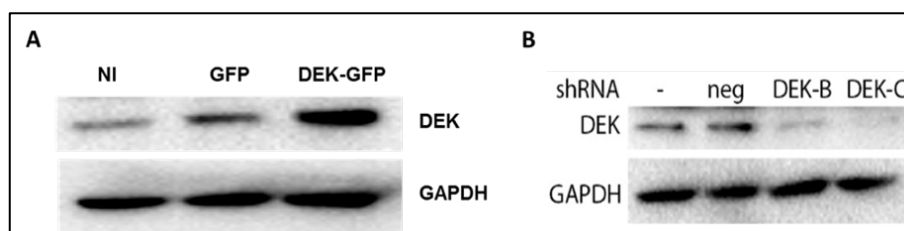


Figure 10.4: Western Blotting results for DEK expression in HS-27A cells with DEK overexpression (A) and downregulation (B).

Altogether, RT-qPCR and Western Blotting analysis results verified stable overexpression and downregulation of DEK expression in HS-27A cells at the mRNA (Figure 10.3) and protein (Figure 10.4) levels. Consequently, verified cells were used to conduct all of the further experiments.

10.3. Analysis of Proliferation Capacity of DEK Overexpressing HS-27A Cells

WST-1 assay was carried out to analyse the effect of DEK overexpression on the proliferation of HS-27A cells. Firstly, culture conditions for HS-27A cells were optimized by seeding cells at different densities. Optimization studies showed that cells reach a plateau on day three when cells are seeded at higher cell densities (Figure 10.5).

As a result, it was decided that the 5×10^3 cells/well of a 96 well plate on day zero provided the best growth curve for 5 consecutive days. This density was used in subsequent cell proliferation and co-culture studies for DEK overexpressing HS-27A cells.

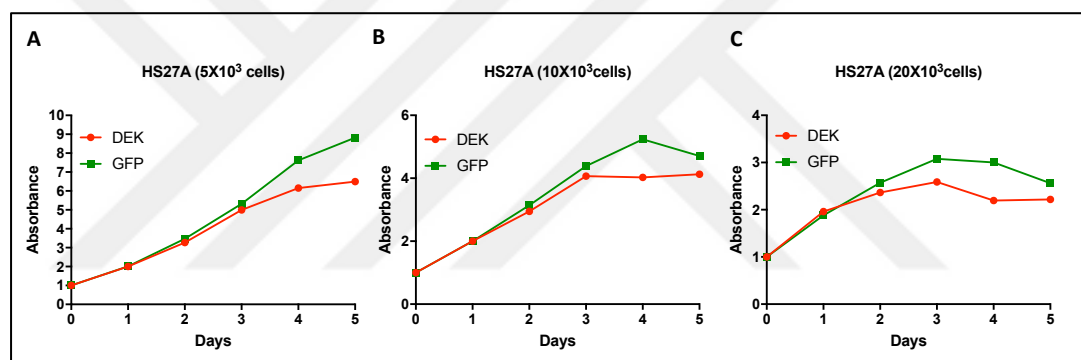


Figure 10.5: Optimization of proliferation conditions for HS-27A-GFP and HS-27A-DEK-GFP cells. Cells were seeded in 96-well plates for each time point and growth curves were obtained by applying WST-1.

WST-1 assay was repeated for HS-27A cells using the cell density of 5×10^3 cells per well. HS-27A-GFP and HS-27A-DEK-GFP cells had similar growth curves for five days; there was only a slight reduction in proliferative capacity of the DEK overexpressing cells at day 4 and 5, which was not statistically significant. Thus, it was determined that DEK overexpression moderately affect the proliferation capacity of HS-27A cells (Figure 10.6).

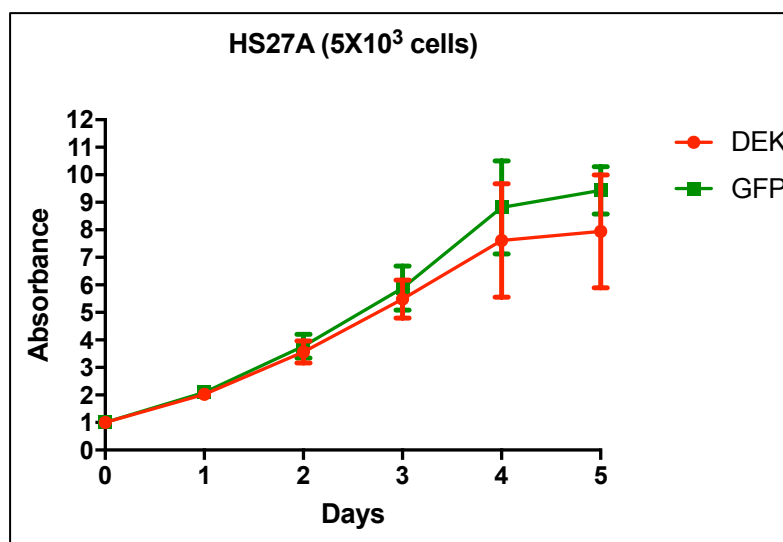


Figure 10.6: Growth curves of HS-27A-GFP and HS-27A-DEK-GFP cells. Cells were seeded in 96-well plates (5×10^3 cells/well) for each time point in triplicates and growth curves were obtained by applying WST-1. Average values of each consecutive day at each sample was divided by the average value of its average day-0 value and these normalized results were shown in the graph. The graph represents the average of two separate experiments (Two-way ANOVA, $P = ns$ (not significant)).

Co-culture studies of MM cells were performed to test whether overexpression of DEK in HS-27A cells influence the proliferation and viability of MM cells. Three approaches that was shown below were followed to assess the effects of the secreted paracrine/autocrine factors or cell-to-cell contacts by adhesion molecules.

10.4.1. Co-Culture with Conditioned Medium (CM)

CM was used to assess the effects of the paracrine factors secreted by HS-27A cells on MM cells. HS-27A cells were cultured in a serum-free medium for 18 hours to obtain CM, including secreted paracrine factors. Initially, growth of the RPMI-8226 (multiple myeloma cell line) cells in the serum-free or serum-containing medium were analyzed by using WST-1 assay. Results showed that RPMI-8226 cells did not proliferate in standard serum-free medium or CM (obtained from HS-27A-GFP and HS-27A-DEK-GFP cells). On the contrary, for cells cultured with 15% serum-containing completed medium, proliferation reached a plateau on day two and decreased after day four (Figure 10.7). Optimization studies showed RPMI-8226 cells

require serum for proliferation and it was decided to add serum to CM in subsequent co-culture studies.

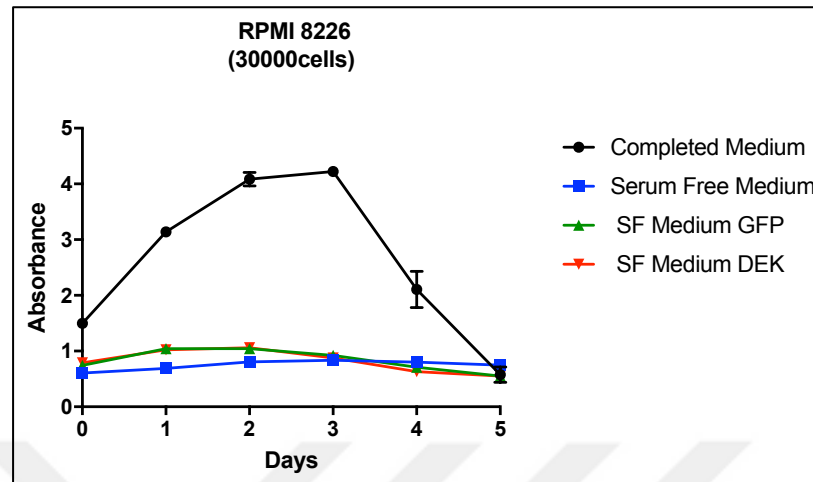


Figure 10.7: Optimization of serum amount for growth curves of RPMI-8226 cells cultured with complete (standard) medium (black line), serum-free medium (blue line) or serum-free CM obtained from HS-27A cells (green and red lines for HS-27A-GFP and HS-27A-DEK-GFP, respectively).

Next, cell density and serum amounts were tested for RPMI-8226 cells. First, a “50%-CM” medium was prepared by adding fresh complete medium (containing 15% serum) to the serum-free CM medium at a 1:1 ratio. Next, RPMI-8226 cells were seeded as 5×10^3 or 3×10^4 in 96-well plates using the “50%-CM” medium. WST-1 assays showed that “50%-CM” was sufficient for the RPMI-8226 cell growth and the density of 5×10^3 cells per well provided the optimal proliferation curve for five consecutive days (Figure 10.8).

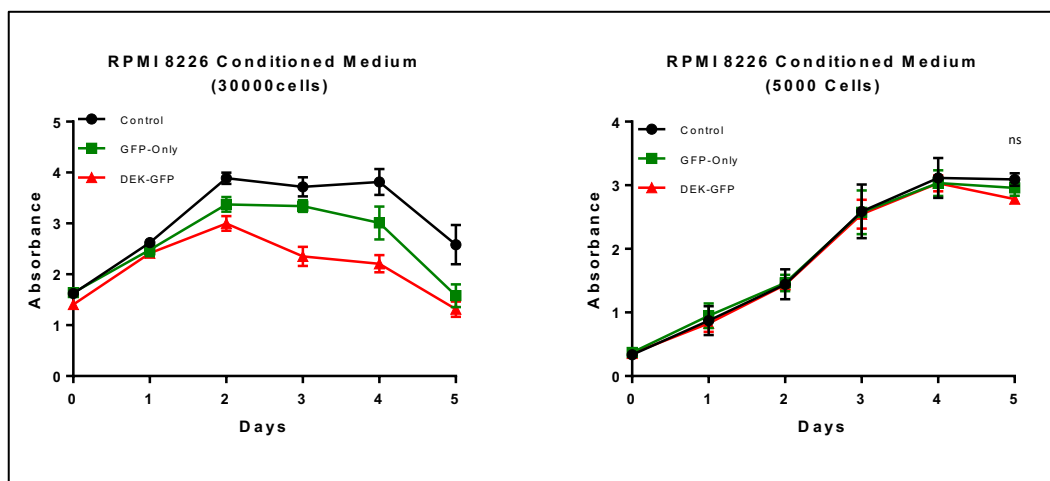


Figure 10.8: Growth curves of RPMI-8226 cells seeded at 5000 cells per well or 30000 cells per well using 50%-CM.

After cell density and serum amount optimization, co-culture experiments with CM were performed for RPMI-8226 and U266 (multiple myeloma cell line) cells using WST-1 assay. RPMI-8226 and U266 cells cultured with CM obtained from HS-27A-DEK-GFP or HS-27A-GFP cells had similar growth curves (Figure 10.9). In conclusion, it was determined that the proliferation of RPMI-8226 or U266 cells is not affected by paracrine factors secreted from DEK overexpressing HS-27A cells.

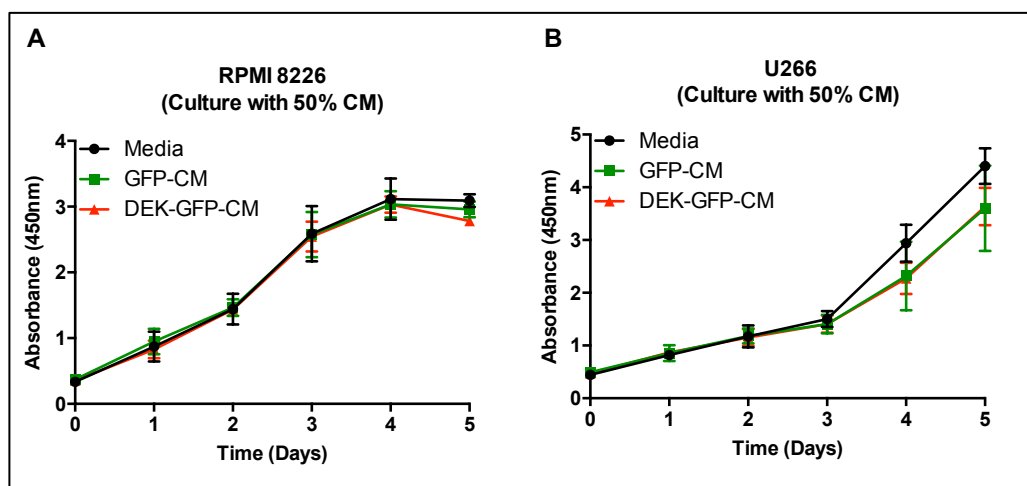


Figure 10.9: Growth curves of RPMI-8226 (A) and U266 (B) cells seeded at a density of 5×10^3 cells/well using CM obtained from HS-27A-GFP and HS-27A-DEK-GFP cells. The graph represents the average of two separate experiments for RPMI 8226 cells and three separate experiments for U266 cells (Two-way ANOVA, $P=ns$ (not significant)).

10.4.2. Indirect Co-Culture

Since co-culture studies using the CM showed no difference for HS-27A cells with DEK overexpression, we tested whether the HS-27A cells need the presence of MM cells to secrete paracrine factors. Therefore, HS-27A and MM cells were cultured in the same well by placing a hanging insert into the 6-well plates. The hanging inserts allow fluid exchange between cells by their pores but prevent direct cell-to-cell interactions. Then, HS-27A cells that were seeded into the hanging insert were discarded and WST-1 assays or trypan blue stainings were performed to evaluate the proliferation of the remaining MM cells. In addition, Annexin-V/FACS analysis was carried out to assess the apoptotic cell rate in RPMI 8226 cells.

WST-1 results for U266 cells (Figure 10.10A) and trypan-blue counts for RPMI 8226 cells (Figure 10.10B) showed that indirect co-culture of HS-27A with DEK overexpression and MM cells, cells has no significant effect on proliferation and viability of MM cells. In addition, Annexin-V/FACS analyses demonstrated that RPMI 8226 cells co-cultured with DEK overexpressing HS-27A cells and control cells have similar apoptotic cell rates (Figure 10.11).

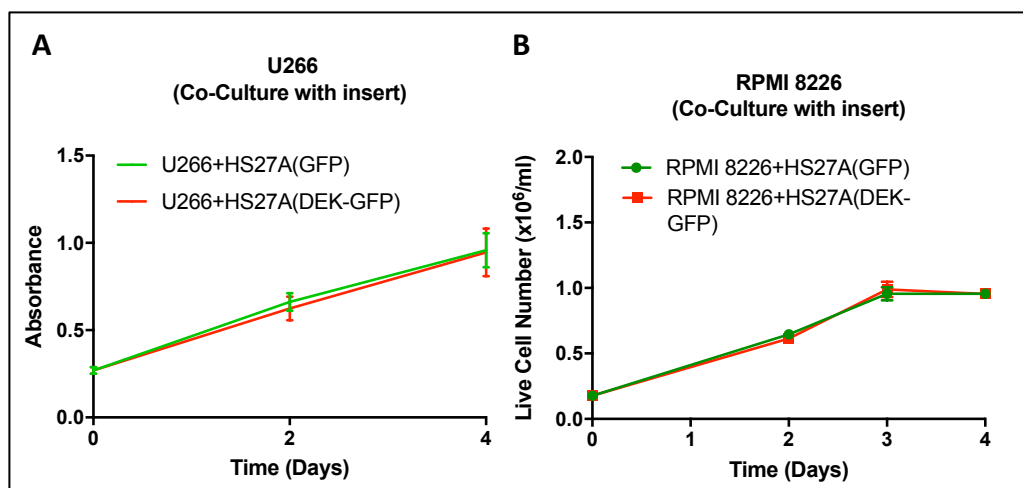


Figure 10.10: Growth curves of U266 (A) and RPMI-8226 (B) cells co-cultured indirectly with HS-27A-GFP and HS-27A-DEK-GFP cells using hanging inserts. The graph represents the average of two separate experiments for RPMI 8226 cells and three separate experiments for U266 cells (Two-way ANOVA, P=ns (non significant)).

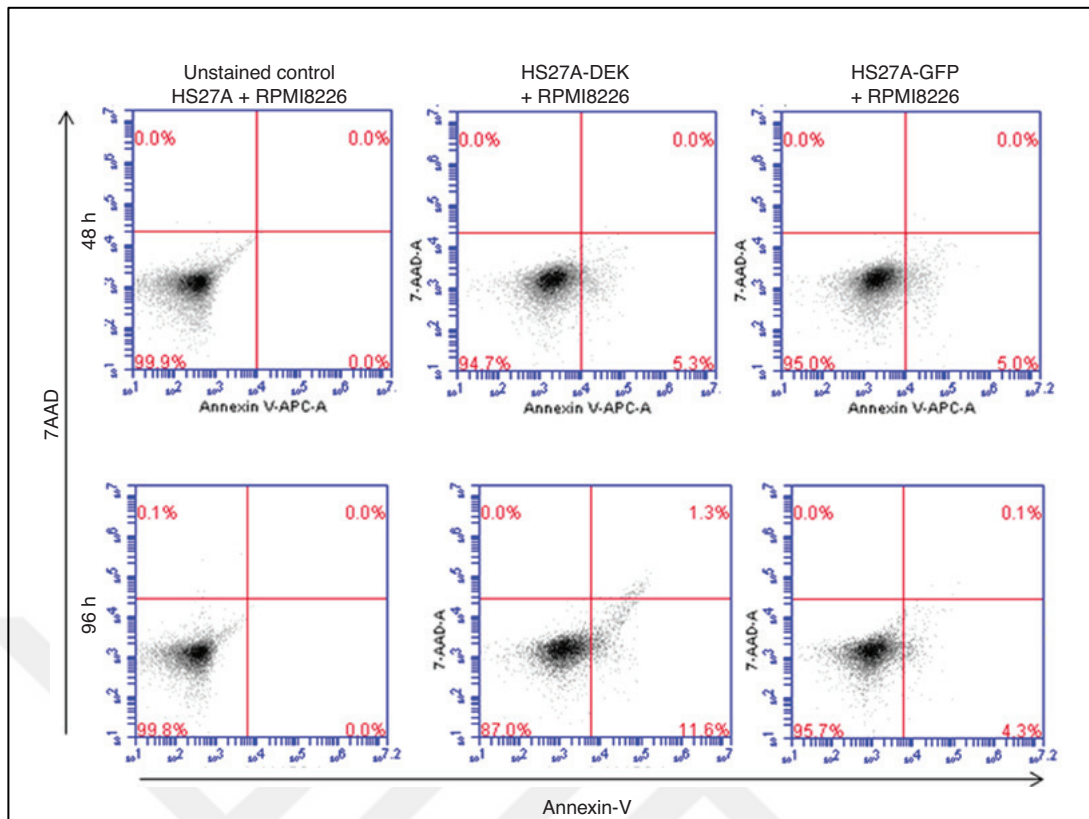


Figure 10.11: Annexin-V analysis of RPMI-8226 cells co-cultured indirectly with HS-27A-GFP and HS-27A-DEK-GFP stroma cells using hanging inserts.

10.4.3. Direct Co-Culture

Finally, effects of the paracrine factors and direct cell-to-cell interactions on cell proliferation were assessed by direct co-culture. HS-27A cells were co-cultured with RPMI-8226 or U266 cells directly in the same well. The proliferation of cells was determined cumulatively by WST-1 or trypan blue countings. Results showed that DEK overexpression in HS-27A cells does not cause any significant effect in the proliferation and viability of MM and HS-27A cells (Figure 10.12).

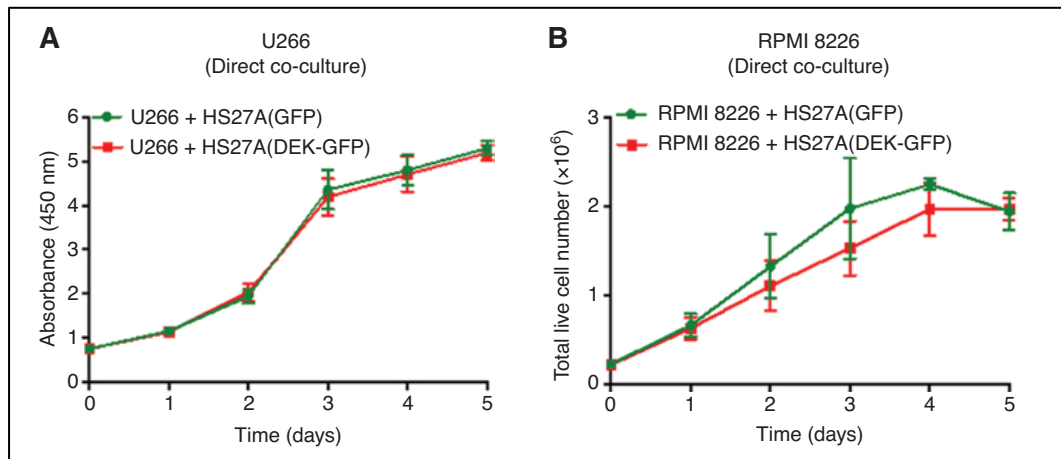


Figure 10.12: Growth curves of U266 (A) and RPMI-8226 (B) cells co-cultured directly with HS-27A-GFP and HS-27A-DEK-GFP stroma cells in the same well. The graph represents the average of two separate experiments (Two-way ANOVA, P=ns, (not significant)).

In conclusion, these results indicated that ectopic DEK expression in HS-27A cells does not significantly affect proliferation, viability, or apoptotic cell rates of the co-cultured MM cells via paracrine or cell-to-cell interactions.

10.5. Determination of Apoptotic Cell Rate in HS-27A Cells after the suppression of DEK expression

After transduction of HS-27A cells with lentiviral vectors, we observed high cell death rates under the microscope. We hypothesized that the induction of apoptosis might cause cell death due to DEK downregulation. To investigate apoptotic cell ratios in HS-27A-shDEK cells, Annexin-V analysis was performed by flow cytometry. Results showed that the Annexin-V⁺ apoptotic cell ratio was 49% and 48% in GFP⁺ HS-27A-shDEK-B and shDEK-C cells, respectively. In GFP⁺ HS-27A-sh-Neg cells, 52% of the cells were Annexin-V⁺ (Figure 10.13). Thus, it was shown that compared to the control (sh-Neg) cells, the apoptotic cell rate was not significantly changed in sh-DEK-expressing HS-27A cells (shDEK-B and shDEK-C).

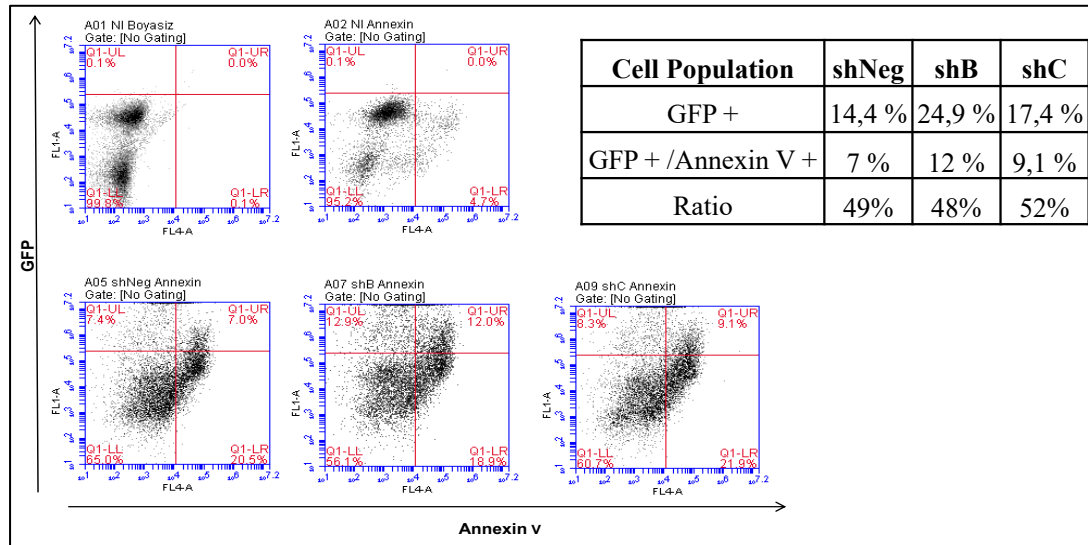


Figure 10.13: Annexin V analysis in control (sh-Neg) and shDEK-expressing (shDEK-B and shDEK-C) cells (left panel) and Annexin-V⁺ cell ratio (right panel).

10.6. Caspase Assay

Upon the induction of apoptosis, inactive pro-caspase proteins are converted into active caspase proteins that proteolytically cleave their target proteins from aspartic acid residues (Chang and Yang, 2000). Apoptosis can take place by two different pathways. The extrinsic pathway is triggered by the initiator caspase-2 or caspase-8 upon the signal outside the cell. Besides, the intrinsic pathway is initiated by caspase-9 as a result of intracellular signals. After initiator caspases are activated, executor caspases (caspase-3 and caspase-6) are cleaved through a protease cascade and the apoptosis signal is propagated further in the cell [Fulda and Debatin, 2006].

The activity of caspase proteins (caspase-2, 3, 6, 8 and 9) was analysed using a caspase assay to reveal the active apoptotic pathways in HS-27A-shDEK cells. Non-infected HS-27A cells were treated with Staurosporine as a positive control for the assay and DMSO was used as a vehicle. Results showed that caspase-2 and caspase-8 activity increased by 2.6 and 6.5-fold in Staurosporine-treated cells. Caspase-9 activity was lower compared to the control cells. Activities of caspase-3 and caspase-6 were increased by 4.8 and 6.6-fold, respectively. Results indicated that Staurosporine successfully triggered apoptosis in HS-27A cells through the external pathway and the assay worked adequately.

On the other hand, HS-27A-shDEK-B cells showed a slight increase (1,6 fold) in caspase 2 activity. Still, no significant difference was detected in the activity of caspase 3, 6, 8 and 9 in DEK downregulated HS-27A cells compared to control cells (Figure 10.14 and Table 10.1). Taken together, our findings showed that DEK downregulation does not affect caspase activity in HS-27A cells.

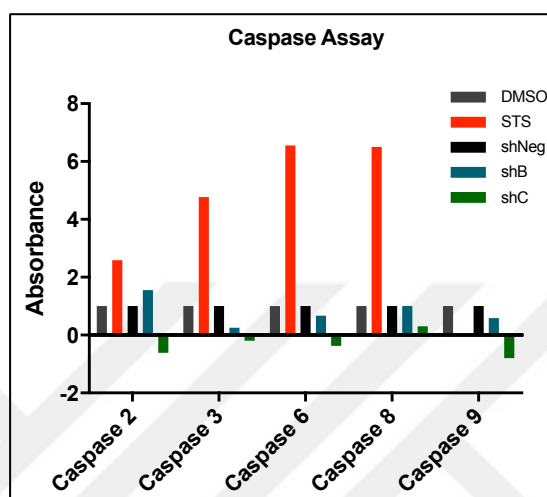


Figure 10.14: Caspase activity in the DEK downregulated HS-27A cells. Parental HS-27A cells were treated with Staurosporine (STS) and its vehicle control DMSO.

Table 10.1: Numerical representation of caspase activity in HS-27A cells with DEK downregulation.

Caspase	DMSO	STS	shNeg	shB	shC
Caspase 2	1	2,6	1	1,6	-0,6
Caspase 3	1	4,8	1	0,3	-0,2
Caspase 6	1	6,6	1	0,7	-0,4
Caspase 8	1	6,5	1	1	0,3
Caspase 9	1	0	1	0,6	-0,8

10.7. MCL-1 and p53 Expression in HS-27A Cells Levels

Anti-apoptotic MCL-1 gene expression was determined at the mRNA level in DEK downregulated HS-27A cells. RT-qPCR results indicated that DEK knockdown does not cause notable alteration in MCL-1 expression (Figure 10.15A).

Additionally, pro-apoptotic p53 gene expression was determined by Western blotting. MDA-MD-231 cells, which permanently express p53, were used as a positive

control. Results showed that p53 protein was not detectable in both control (sh-neg) and DEK knockdown HS-27A cells (sh-B and sh-C) (Figure 10.15B). These results suggested that MCL-1 and p53 expressions in HS-27A cells were not significantly affected by DEK downregulation.

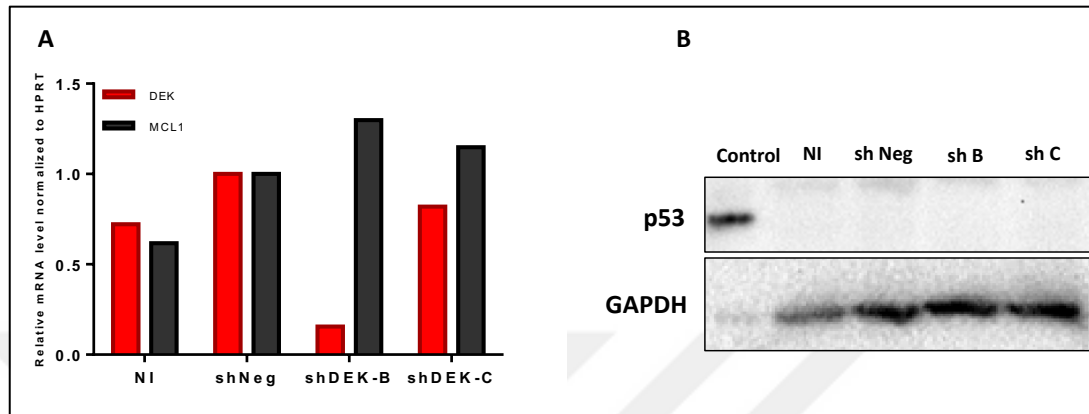


Figure 10.15: Expression of MCL-1 (A) and p53 (B) in HS-27A cells with downregulated DEK expression. MDA-MD-231 cells were used as positive control in panel B.

10.8. Dilution of Virus Medium for Lentiviral Transduction of HS-27A Cells

Our previous results showed apoptotic pathways were not activated in HS-27A cells after transduction with lentiviral vectors. Then, we thought that cell death may be caused by high levels of sh-RNA expression in cells rather than DEK downregulation. In subsequent transduction, the virus medium was diluted at 1/6 and 1/10 ratios to reduce sh-RNA expression level in the HS-27A cells. Cell viability and transduction efficiency was evaluated under the microscope and by flow cytometry analysis. Results showed that GFP⁺ cell ratios were high for both dilutions, but 1/6 dilution provided even higher transduction efficiency (Figure 10.16). FACS-sort was not required because of the already high GFP⁺ cell ratios and cells were used as such in the following experiments.

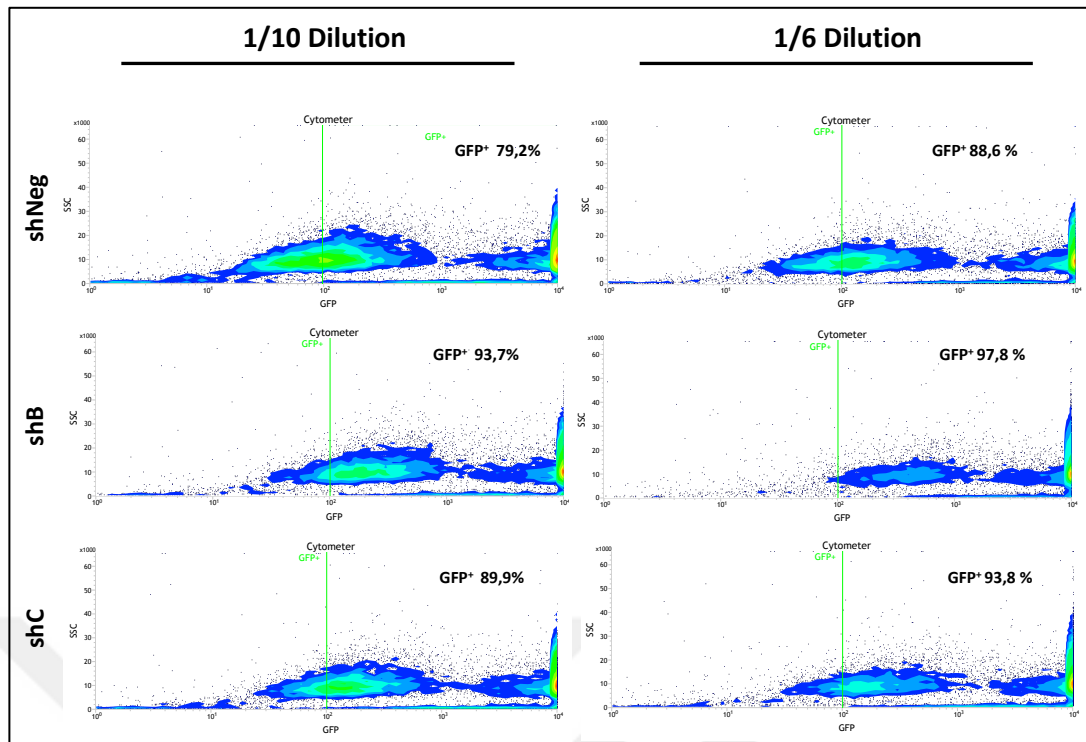


Figure 10.16: GFP analysis after lentiviral transduction of HS-27A cells by diluting virus medium as 1/6 and 1/10.

RT-qPCR results revealed that DEK was suppressed by 34% in HS-27A-shDEK-B cells for 1/10 dilution. However, no decrease in DEK expression was detected in HS-27A-shDEK-C cells compared to the control cells. Besides, when 1/6 virus dilution was used, expression of endogenous DEK was downregulated by 65% and 36% in the HS-27A shDEK-B and HS-27A shDEK-C cells, respectively (Figure 10.17). Therefore, it was decided that 1/6 dilution was ideal to avoid the toxic effect of strong shRNA expression in HS-27A cells and this dilution rate provides sufficient downregulation of DEK expression. Those cells were used in the following experiments.

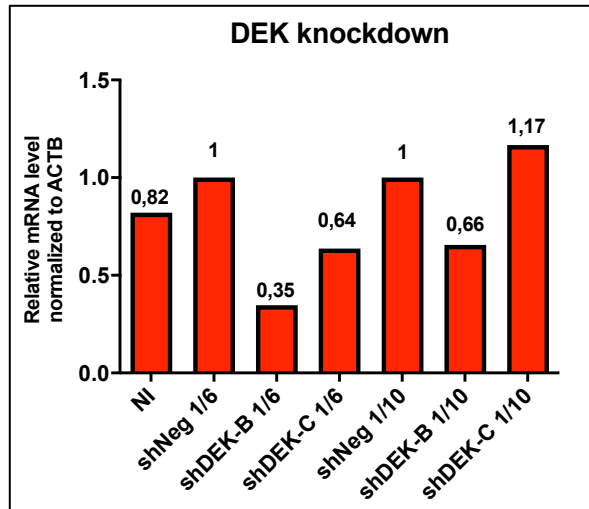


Figure 10.17: RT-qPCR analysis for the confirmation of DEK expression at mRNA level after transduction of HS-27A cells by diluting the virus medium at 1/6 and 1/10 ratios.

10.9. WST-1 Proliferation Assay of DEK Downregulated HS-27A Cells

The proliferation of HS-27A cells with downregulated DEK expression was investigated by WST-1 assay. Cells were seeded at different densities and growth curves were obtained for five consecutive days. The results showed that HS-27A shNeg and HS-27A shDEK-C cells had similar growth curves for five days but there was a slight reduction in proliferative capacity of the HS-27A shDEK-B cells. Thus, it was determined that DEK downregulation moderately affect the proliferation capacity of HS-27A cells (Figure 10.18).

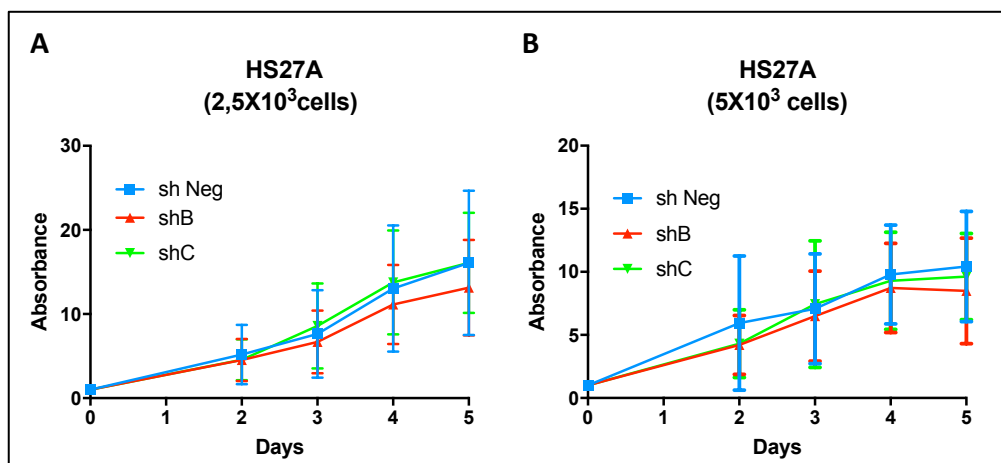


Figure 10.18: Growth curves of HS-27A cells seeded as $2,5 \times 10^3$ or 5×10^3 cells per well. Cells were seeded in 96-well plates (5×10^3 cells/well) for each time point in triplicates and growth curves were obtained by applying WST-1. Average values of each consecutive day at each sample was divided by the average value of its average day-0 value and these normalized results were shown in the graph. The graph represents the average of two separate experiments (Two-way ANOVA, $P = ns$ (not significant)).

10.10. Wound Healing Assay for HS-27A Cells

To examine the migration of HS-27A cells with DEK modification, wound-healing assay was performed. Initially, a wound-like cell-free space was created by drawing a line along the cell surface with a 10 μ l or 200 μ l pipette tip and the cell-free space was monitored for 24 hours. After 24 hours, cell-free space was closed entirely in the wound generated by a 10 μ l tip. Cell-free space was also heavily occupied in the wound generated using a 200 μ l-tip. Therefore, the image acquisition time was decided to be before 24 hours. Additionally, 200 μ l pipette tip was selected as the appropriate pipette tip for wound creation (Figure 10.22)

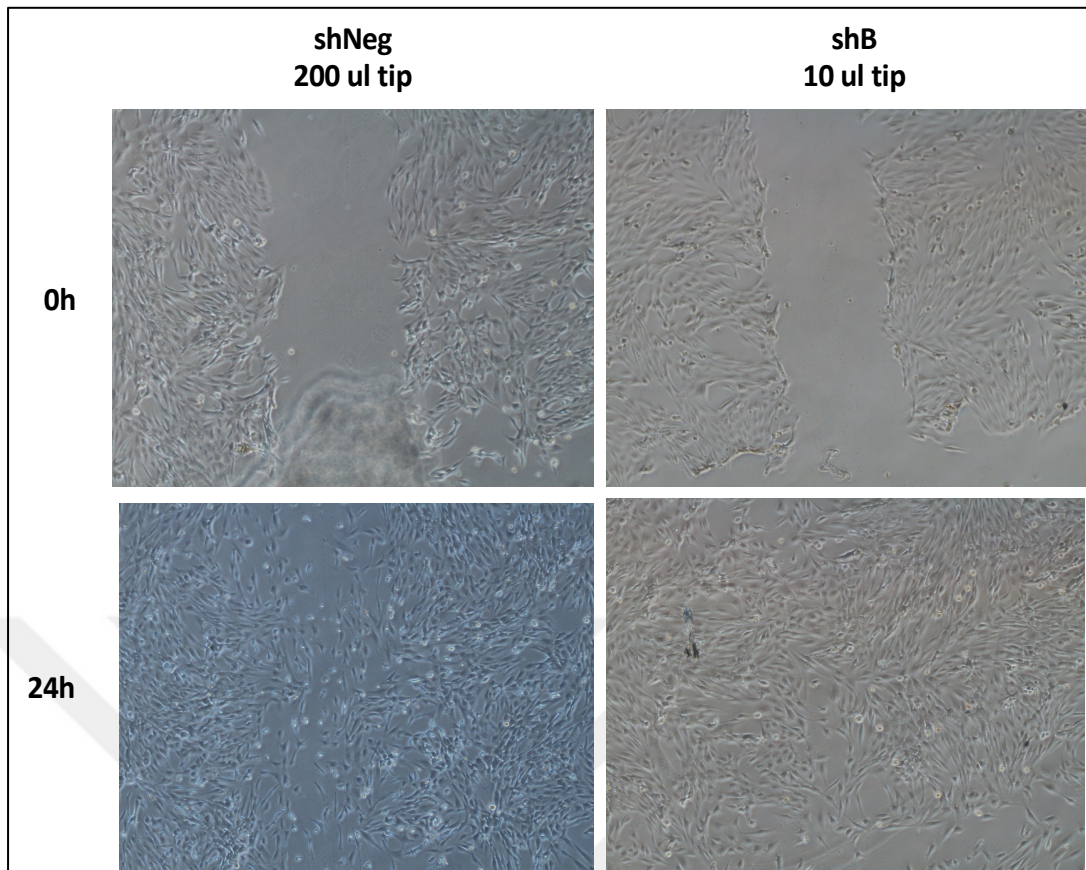


Figure 10.22: Images for wounds created using 200 μ l and 10 μ l pipette tips for HS-27A shNeg and HS-27A sh-DEK-B cells at 0h and 24 h (Eclipse Ti-S, Nikon, Magnification 4X).

After optimization studies, wound healing assays were performed with HS-27A-DEK-GFP and HS-27A-shDEK cells and wound closure rates were analyzed using ImageJ software. Under the experimental conditions that we used, results demonstrated that knockdown or overexpression of DEK in HS-27A cells affected migration capacity similarly similar (Figures 10.23,10.24 and 10.25).

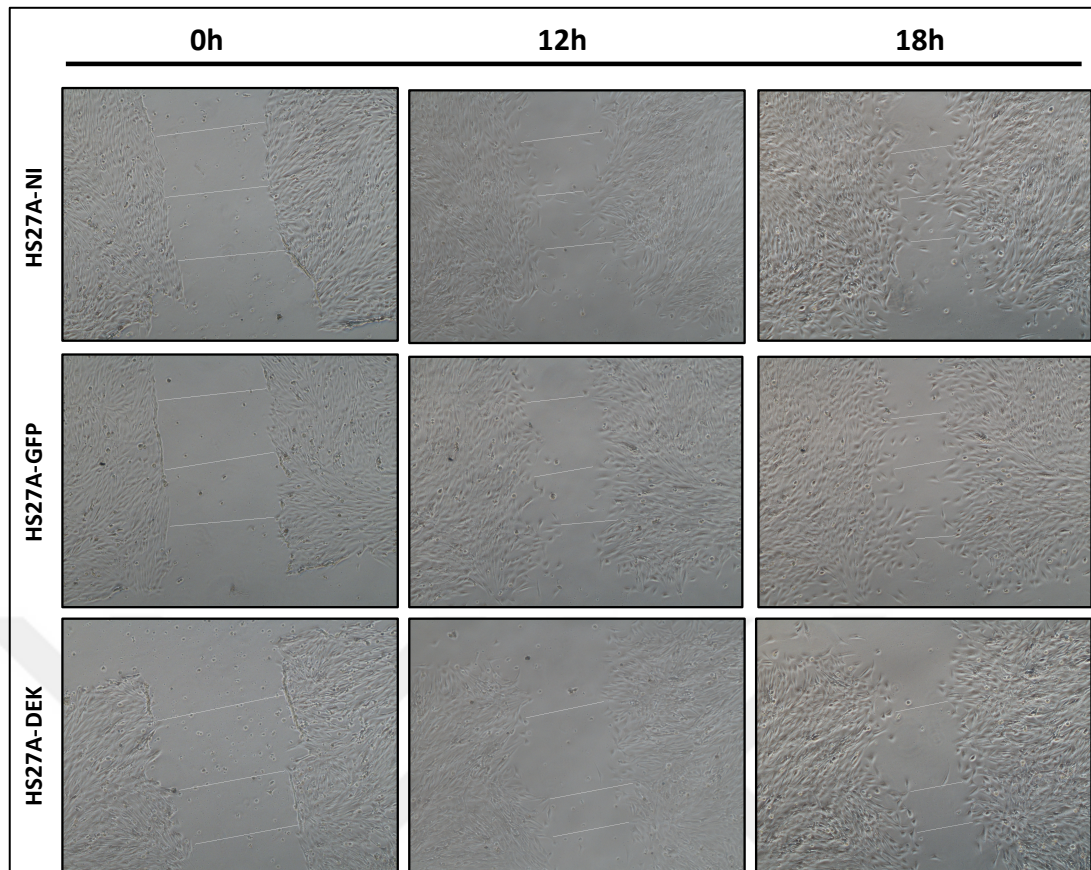


Figure 10.23: Wound closure after 0, 12 and 18 hours for HS-27A NI, HS-27A GFP, HS-27A DEK-GFP cells (Eclipse Ti-S, Nikon, Magnification 4X).

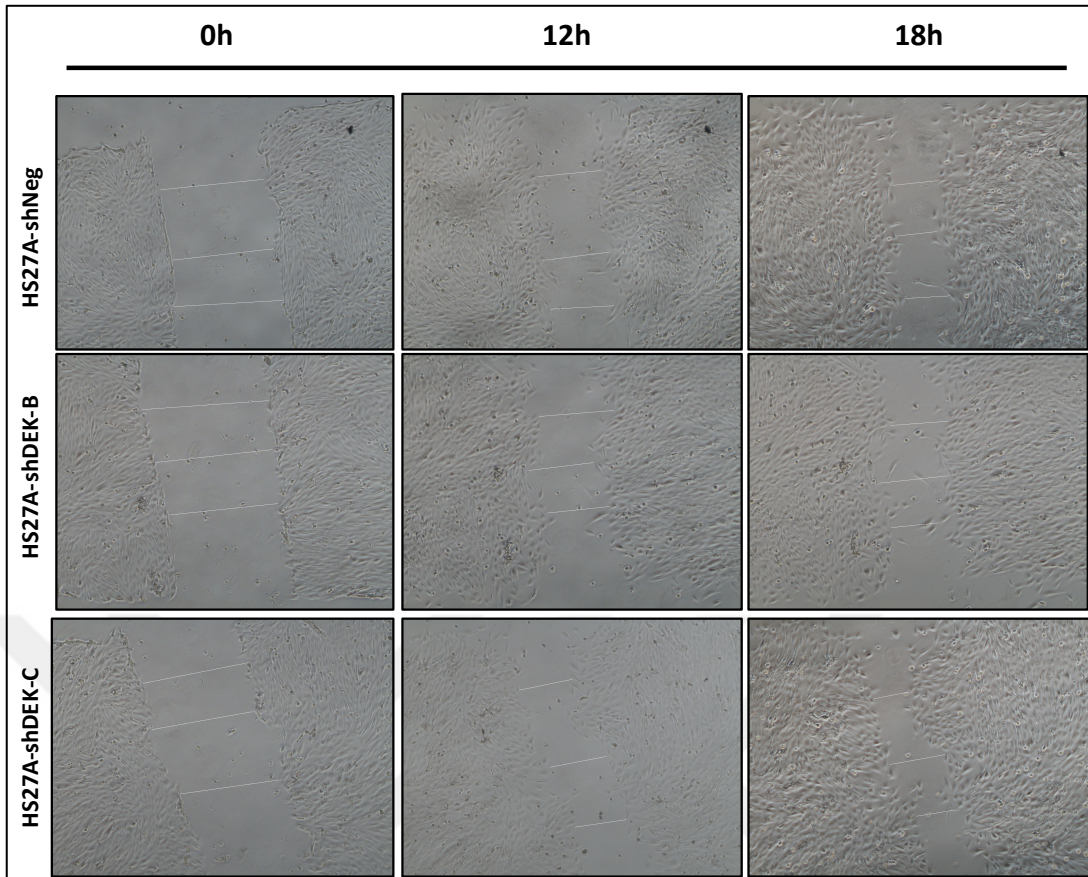


Figure 10.24: Wound closure after 0, 12 and 18 hours for HS-27A NI, HS-27A GFP, HS-27A DEK-GFP cells (Eclipse Ti-S, Nikon, Magnification 4X).

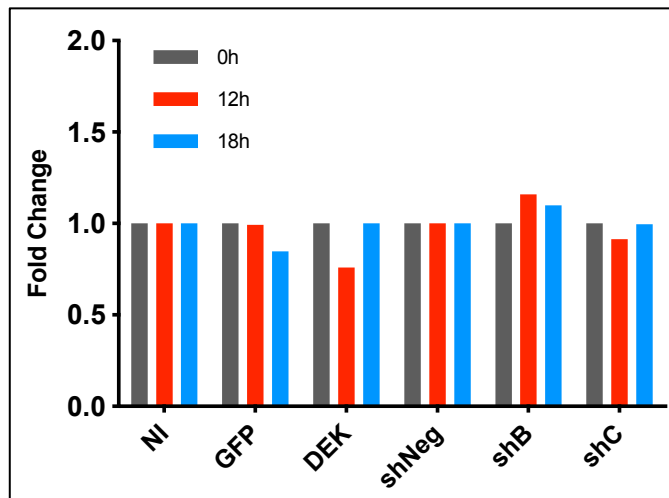


Figure 10.25: Graphical representation of wound closure rates of HS-27A cells.

10.11. Modification of DEK Expression in HS-5 Cells

To evaluate the effects of DEK expression on IL-6 secretion, DEK expression was modified in HS-5 cells because of their higher IL-6 expression compared to HS-27A cells. DEK expression was overexpressed in HS-5 cells by retroviral transduction and cells were sorted by FACS analysis. Flow cytometry analysis revealed that GFP⁺ cell ratios were 91% and 60% for HS-5-GFP and HS-5-DEK-GFP cells, respectively (Figure 10.26). Since the transduction efficiency was insufficient for HS-5-DEK-GFP, cells were sorted again and GFP⁺ cell ratio for HS-5-DEK-GFP reached to 90% (Figure 10.27).

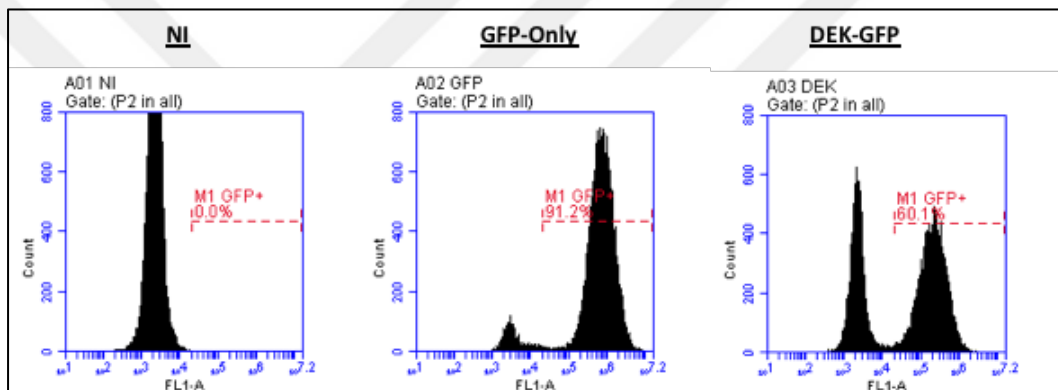


Figure 10.26: GFP analysis of HS-5 cells after FACS sorting of retrovirally transduced cells.

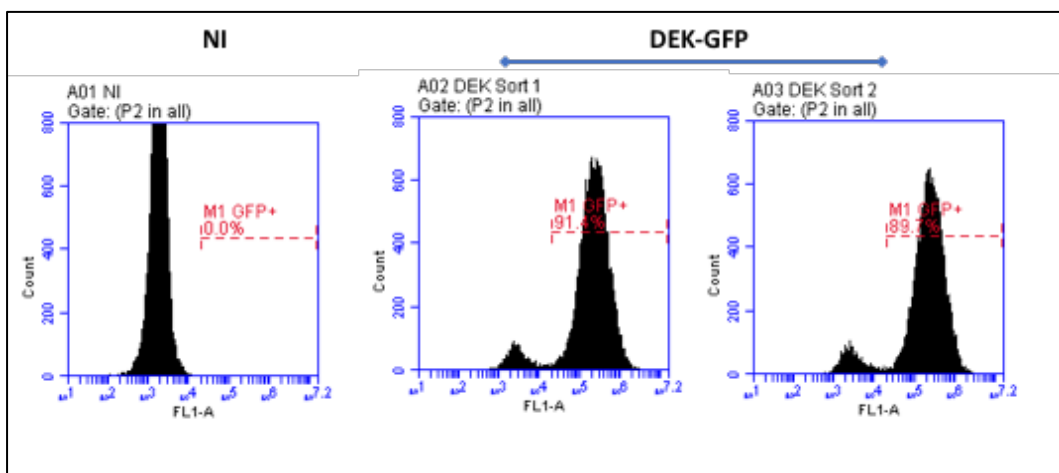


Figure 10.27: GFP analysis of HS-5-DEK-GFP cells after second FACS sorting.

DEK expression was also suppressed in HS-5 cells using the same sh-DEK lentiviral constructs. Upon the lentiviral transduction, HS-5 cells were sorted by FACS. GFP⁺ cell ratios were 87% and 94% in HS-5-sh-DEK-B and sh-DEK-C cells, respectively. For HS-5-sh-Neg cells, 86% of cells were GFP⁺ (Figure 10.28). Therefore, sorted HS-5 cells were used as such in subsequent experiments.

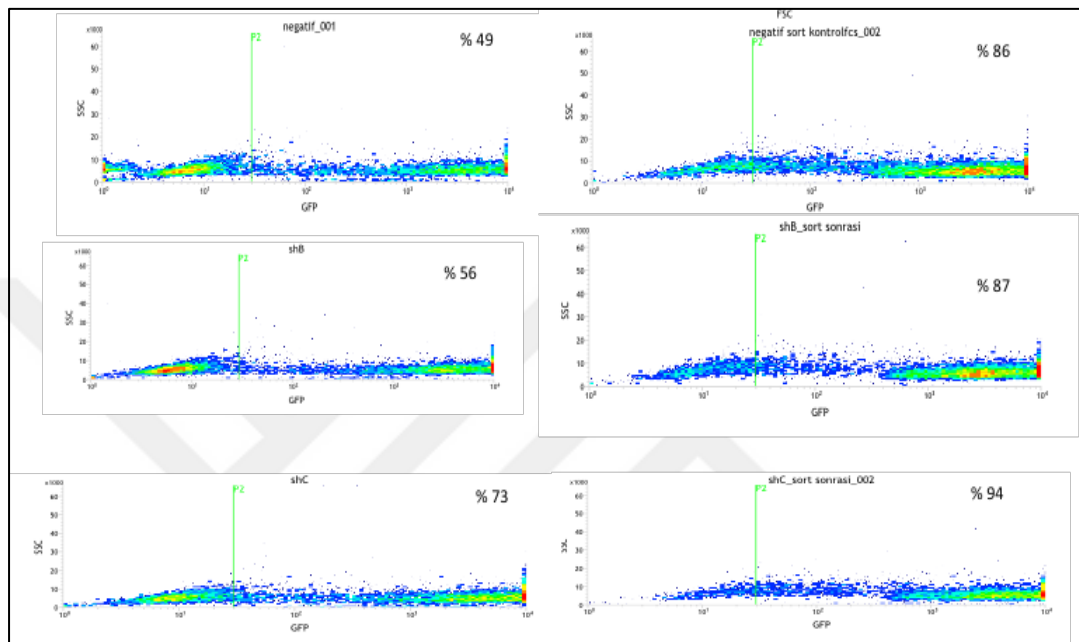


Figure 10.28: FACS analysis result after lentiviral transduction of HS-5 cells. GFP analysis result of control HS-5 sh-Neg cells before (A) and after (B) sorting, sh-B cells before (C) and after (D) sorting, and sh-C cells before (E) and after (F) sorting.

10.12. Confirmation of DEK Expression in HS-5 Cells

RT-qPCR and Western Blotting were used to verify whether the modification of DEK expression in HS-5 cells was successful. Results indicated that HS-5-DEK-GFP cells had an approximately 3-fold increase in DEK expression compared to the control cells (Figure 10.29A). On the other hand, DEK mRNA was suppressed by 80% and 50% in HS-5-shDEK-B and HS-5-shDEK-C cells, respectively (Figure 10.29B). Furthermore, Western Blotting results demonstrated that DEK bands in the cell lysates of HS-5-shDEK-B cells were weaker than HS-5-shNeg cells and parental cells (Figure 10.29C). HS-5-shDEK-C cells showed no decrease for DEK expression at the protein level, which was contrary to the mRNA results. Thus, the mRNA and protein levels

confirmed stable overexpression, and downregulation of DEK in HS-5-shDEK-B cells.

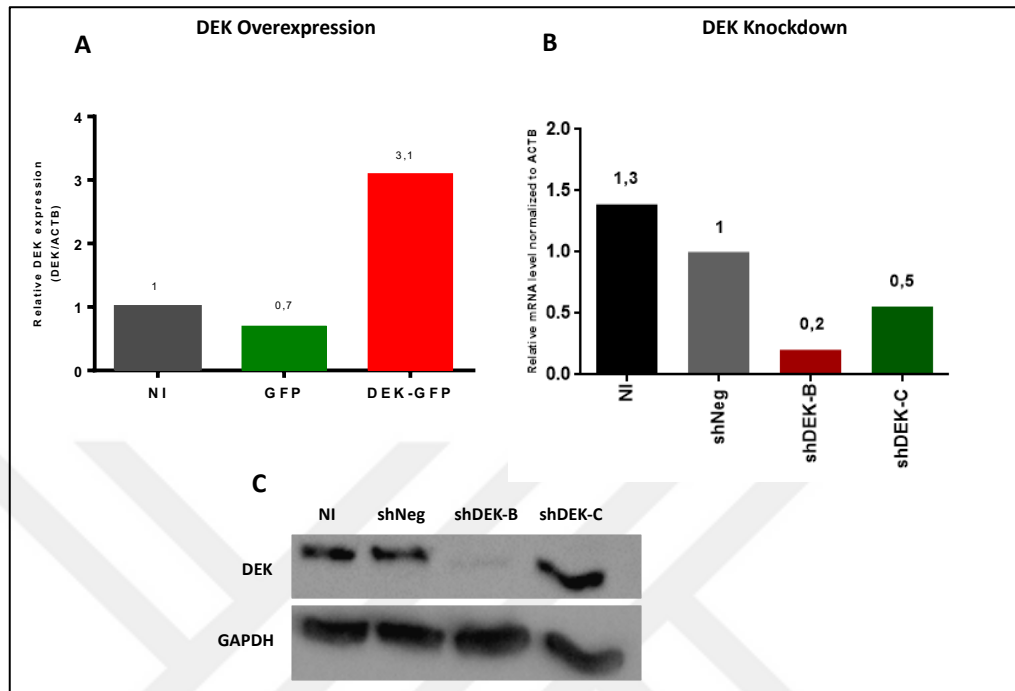


Figure 10.29: Confirmation of DEK overexpression (A) or downregulation (B and C) in HS-5 cells by RT-qPCR or Western Blotting.

10.13. Determination of IL-6 Expression in HS-5 Cells

IL6 expression in HS-5 cells with modified DEK expression was determined at the mRNA and protein levels. RT-qPCR results showed that IL-6 expression increased slightly (3,1 fold) in HS-5-DEK-GFP cells compared to HS-5-GFP control cells. On the other hand, HS-5-shDEK-B and HS-5-shDEK-C cells had a 50% and 40% decrease in IL-6 mRNA level, respectively, compared to HS-5-shNeg control cells (Figure 10.30A). Western Blot results demonstrated that the IL-6 expression was higher in HS-5-DEK-GFP cells compared to the HS-5-GFP cells. Additionally, level of IL-6 was lower in the HS-5-shDEK-B than HS-5-shNeg cells. HS-5-shDEK-C cells had no decrease in the protein level of IL-6, contrary to the mRNA results (Figure 10.30B). These data suggested that DEK expression positively affects IL-6 expression in HS-5 cells.

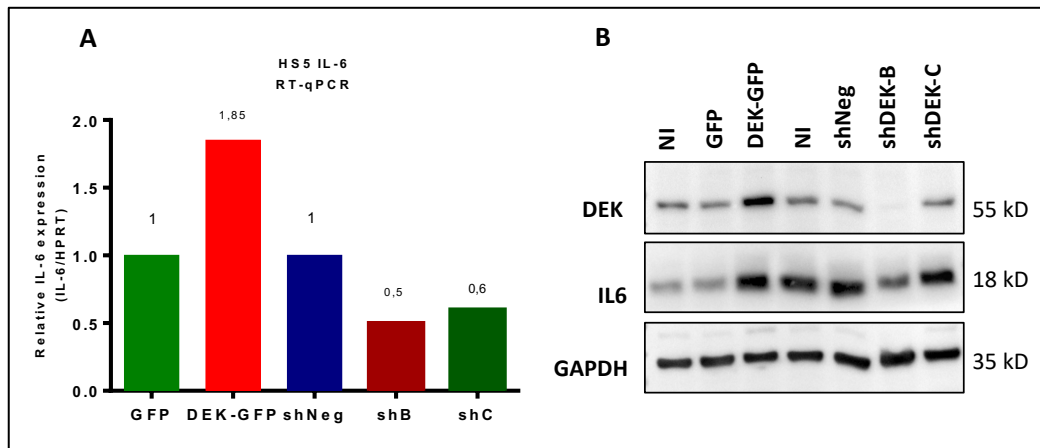


Figure 10.30: IL-6 expression in HS-5 cells at the mRNA (A) and protein (B) levels.

10.14. Analysis of IL-6 Secretion in the HS-5-shDEK Cells

Next, we wanted to evaluate IL-6 secretion in HS-5 cells with DEK downregulation. Towards this aim, different medium amounts (1000 μ l, 500 μ l and 250 μ l) conditioned medium was collected from HS-5-shDEK cells and precipitated by using TCA. Additionally, cell lysates were analyzed to verify endogenous DEK and IL-6 protein expression in cells. Results showed that IL-6 bands for 1000 μ l and 250 μ l were weaker for HS-5-shDEK-B than control shNeg bands. However, this correlation was not observed for 500 μ l bands, possibly due to unequal loading of the samples. Additionally, DEK, which is known to be secreted from macrophages, was not detected in the medium of unmodified HS-5 cells. Bands belonging to cell lysates verified the downregulation of DEK and IL-6 in HS-5-sh-DEK-B (Figure 10.31). In conclusion, these results suggested that secretion of IL-6 may also be affected by the DEK gene alteration in HS-5 cells in addition to its endogenous expression.

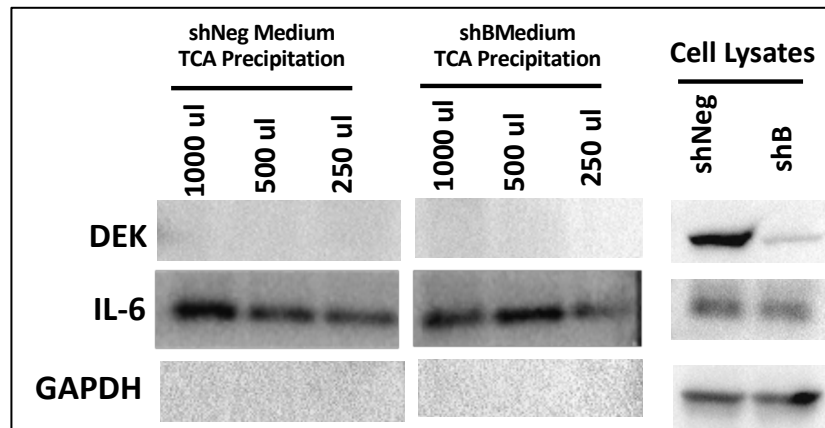


Figure 10.31: Detection of secreted IL6 in the medium of HS-5-shDEK-B cells.

10.15. Cytokine Array

The secretion of 105 cytokines was investigated by using cytokine array in HS-5 cells with altered DEK expression. Results showed that angiogenin, CXCL10 and YKL-40 secretion increased by 70%, 40% and 40%, respectively, in HS-5-DEK-GFP cells compared to HS-5-GFP cells (Figure 10.32A and B). Besides, angiogenin, CXCL10 and YKL-40 secretion were decreased by 40%, 50% and 40%, respectively, in HS-5-shDEK-B cells compared to HS-5 sh-Neg cells (Figure 10.32C and D). In terms of IL-6 secretion, a significant difference couldn't be detected by cytokine array in HS-5-DEK-GFP or HS-5-shDEK-B cells. In conclusion, cytokine array results revealed that there might be a mild correlation between DEK expression and secretion of angiogenin, CXCL-10 and YKL-40 proteins in HS-5 cells.

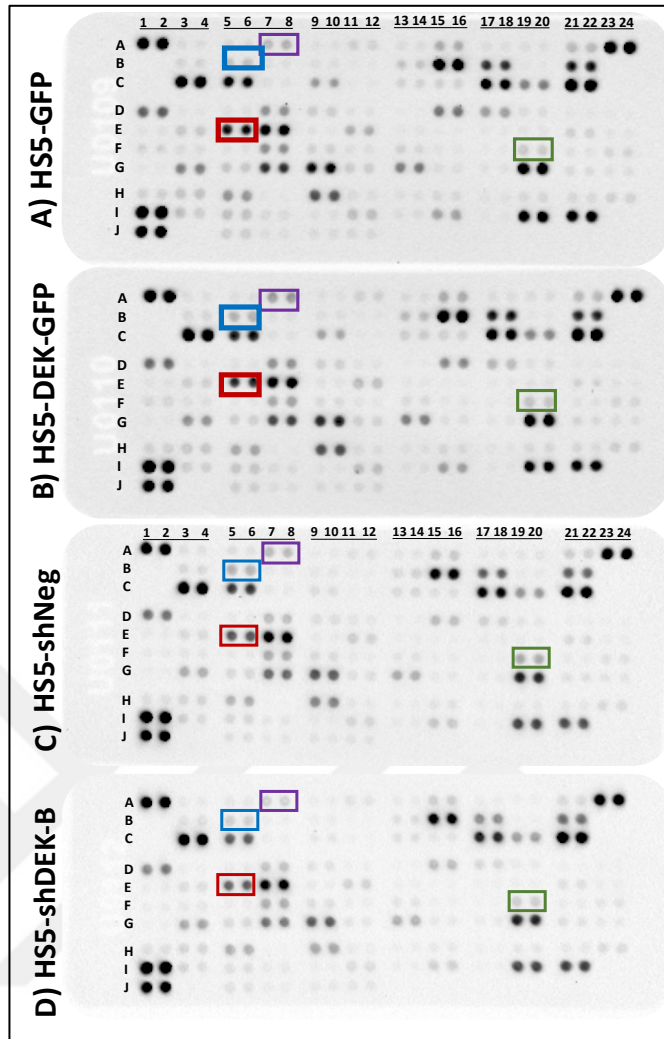


Figure 10.32: Cytokine secretion profile in HS-5 cells altered DEK expression. Angiogenin (A7-8, purple rectangular), YKL-40 (B5-6, blue rectangular) and CXCL10 (F19-20, green rectangular), IL6 (E5-6, red rectangular) were indicated in the array.

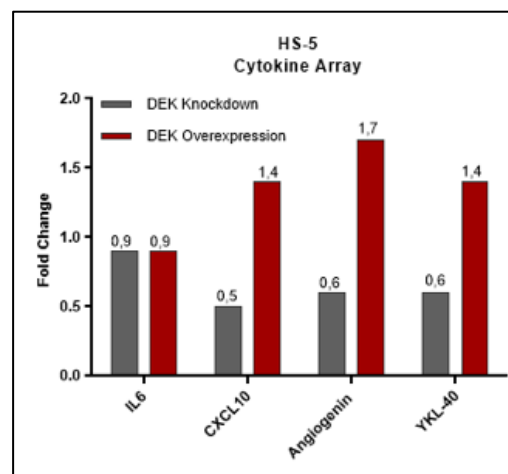


Figure 10.33: Graphical representation of cytokine array results.

11. DISCUSSION

Similar to many other malignancies, the BM microenvironment influences the proliferation, survival and chemoresistance of MM cells. DEK, known as a proto-oncogene, is overexpressed in many solid tumor tissues. In our previous studies, we showed that DEK expression was increased over 2-fold in BM microenvironment of several MM patients. However, the effect of alterations in DEK expression in BM microenvironment cells remains elusive. Considering the significance of the BM microenvironment in MM development, it is vital to comprehensively investigate the possible impacts of alterations in DEK expression detected in the BM on the biology of cells.

In this thesis, our goal was to analyze the effect of altered DEK expression in BM stromal cells on the proliferation, viability and chemoresistance of MM cells. For this purpose, DEK expression in human BM stromal cell lines (HS-27A or HS-5 cells) was overexpressed using retroviral vectors or downregulated with lentiviral sh-RNA vectors. The short-term proliferation capacities of DEK-modified HS-27A cells were evaluated using WST-1 assay. In addition, wound healing assay was conducted to observe migration of stromal cells with modified DEK expression.

Furthermore, HS-27A cells with DEK overexpression were co-cultured with MM cell lines (RPMI-8226 and U266) using three different approaches (CM, direct or indirect co-culture methods). Their effects on MM cell proliferation and viability were evaluated by WST-1 assay or trypan blue counting. Flow cytometry analysis was conducted to analyse apoptosis rates of MM cells co-cultured with BM stromal cells using Annexin V staining. Additionally, the impact of altered DEK expression on cytokine secretion HS-5 cells was assessed by cytokine array and TCA precipitation.

Confirmation of DEK expression by RT-qPCR or Western Blotting showed that DEK was successively overexpressed and down-regulated in bone marrow stromal cell lines. However, it has been observed that DEK overexpression or downregulation only moderately slowed the short-term proliferation of HS-27A cells. In addition, wound healing assay results indicated that the migration capacity of HS-27A cells is not altered because of the modifications of the DEK expression. It is important to note that, using lower amount of serum in the culture and then following the migration of the cells in additional time points would be considered in future since lowering the

amount of the serum could allow better discrimination of migration effect from the proliferation of the cells.

Co-culture studies demonstrated that DEK overexpression in HS-27A cells does not influence the proliferation and viability of the MM cells significantly. Additionally, apoptotic cell rates were similar in the MM cells co-cultured with DEK overexpressing HS-27A cells compared to control cells.

Western Blot analysis showed that DEK overexpression or knockdown leads to increased or decreased IL-6 expression in the HS-5 cells. Similarly, TCA results indicated a positive correlation between IL-6 secretion and DEK expression in HS-5 cells. Interestingly, we could not detect DEK secretion in HS-5 cells by TCA precipitation. In addition, cytokine array results indicated that DEK expression in HS-5 cells slightly affects ANG, CXCL10 and YKL-40 secretion, which are essential proteins involved in hematopoiesis or carcinogenesis. Further studies are required to verify these findings using other methods.

Under the experimental conditions used in this thesis, our findings demonstrated that overexpression or downregulation of DEK expression only moderately affect the proliferation but not viability or migration of bone marrow stromal cells HS-27A. Additionally, it was observed that proliferation and viability of MM cells is not significantly affected by DEK expression in BM stromal cells. However, it is shown that modification of DEK expression might influence cytokine expression and secretion profile of the BM stromal cells.

Other groups observed that IL-6 levels are elevated in the serum of MM patients [Solary et al., 1992], [Stephens et al., 2012]. Additionally, it was indicated that DEK downregulation affects the expression of genes related to the immune system, including IL6 in Squamous Cell Head and Neck Cancer cell lines [Adams et al., 2015]. Another study demonstrated that the increase in expression of DEK was reflected in IL-6 expression in Oropharyngeal Squamous Cell Carcinoma cells [Smith et al., 2017].

Similarly, we showed that DEK expression has an impact on cytokine expression of the BM stromal cells. Considering our previous findings showing DEK overexpression in the BM microenvironment of MM patients, we suggest that DEK expression affects the cytokine secretion of BM stromal cells, which may alter the BM microenvironment. Further experiments are required to reveal the impact of DEK modifications in the bone marrow microenvironment. Additionally, elucidating how DEK controls cytokine expression in the BM microenvironment is vital to

understanding the biology of the BM microenvironment. Eventhough we downregulated of DEK in sh-DEK-B cells strongly, knockout DEK models can be generated using CRISPR-Cas9 system or other techniques and role of DEK can be evaluated in full knockout or conditional knockout models. RNA-seq or mass spectrometry data from those models can be used to screen possible targets of DEK for cytokine secretion in BM stromal cells. Regarding the effect of the BM microenvironment on the development, proliferation and drug resistance of cancer cells, we believe these findings show potential contributions of DEK expression in the development and progression of MM via altering the BM microenvironment.

This study is funded by the TÜBİTAK grants (KBAG-212T108 and 118Z664) and GTU-BAP-2017-A105-40 grant.



REFERENCES

- Adams A.K., Bolanos L.C., Dexheimer P.J., Karns R.A., Aronow B.J., Komurov K., Jegga A.G., Casper K.A., Patil Y.J., Wilson K.M., (2015), "IRAK1 is a novel DEK transcriptional target and is essential for head and neck cancer cell survival", *Oncotarget*, 6, 43395-43407.
- Anthony B.A., Link D.C., (2014), "Regulation of hematopoietic stem cells by bone marrow stromal cells", *Trends Immunol*, 35, 32-37.
- Avalos A.M., Ploegh H.L., (2014), "Early BCR Events and Antigen Capture, Processing, and Loading on MHC Class II on B Cells." *Front Immunol*, 5, 92.
- Avet-Loiseau H., Attal M., Moreau P., Charbonnel C., Garban F., Hulin C., Leyvraz S., Michallet M., Yakoub-Agha I., Garderet L., (2007), "Genetic abnormalities and survival in multiple myeloma: the experience of the Intergroupe Francophone du Myelome", *Blood*, 109, 3489-3495.
- Bergsagel P.L., Chesi M., Nardini E., Brents L.A., Kirby S.L., Kuehl W.M., (1996), "Promiscuous translocations into immunoglobulin heavy chain switch regions in multiple myeloma", *Proceedings of the National Academy of Sciences of the United States of America*, 93, 13931-13936.
- Burrows P.D., Suematsu S., Watanabe T., (2000), "Activation of self-reactive B cells and autoimmune diseases", *Rev Immunogenet*, 2, 38-51.
- Caliskaner Z.O., Cakar T., Ozcelik E., Ozdilek A., Kim A.S., Dogan O., Bosompem A., Grosveld G., Saka B., Kandilci A., (2017), "DEK protein level is a biomarker of CD138positive normal and malignant plasma cells", *PLoS One*, 12, e0178025.
- Cambier J.C., Gauld S.B., Merrell K.T., Vilen B.J., (2007), "B-cell anergy: from transgenic models to naturally occurring anergic B cells?", *Nat Rev Immunol*, 7, 633-643.
- Carro M.S., Spiga F.M., Quarto M., Di Ninni V., Volorio S., Alcalay M., Muller H., (2006), "DEK Expression is controlled by E2F and deregulated in diverse tumor types", *Cell Cycle*, 5, 1202-1207.
- Chesi M., Bergsagel P.L., (2013), "Molecular pathogenesis of multiple myeloma: basic and clinical updates", *Int J Hematol*, 97, 313-323.
- Crowley L.C., Marfell B.J., Christensen M.E., Waterhouse N.J., (2016), "Measuring Cell Death by Trypan Blue Uptake and Light Microscopy", *Cold Spring Harb Protoc* 2016.
- D'Souza L., Bhattacharya D., (2019), "Plasma cells: You are what you eat", *Immunol Rev*, 288, 161-177.

Dankbar B., Padro T., Leo R., Feldmann B., Kropff M., Mesters R.M., Serve H., Berdel W.E., Kienast J., (2000), "Vascular endothelial growth factor and interleukin-6 in paracrine tumor-stromal cell interactions in multiple myeloma", *Blood*, 95, 2630-2636.

Derenne S., Monia B., Dean N.M., Taylor J.K., Rapp M.J., Harousseau J.L., Bataille R., Amiot M., (2002), "Antisense strategy shows that Mcl-1 rather than Bcl-2 or Bcl-x(L) is an essential survival protein of human myeloma cells", *Blood*, 100, 194-199.

Doulatov S., Notta F., Laurenti E., Dick J.E., (2012), "Hematopoiesis: a human perspective", *Cell Stem Cell*, 10, 120-136.

Evans A.J., Gallie B.L., Jewett M.A., Pond G.R., Vandezande K., Underwood J., Fradet Y., Lim G., Marrano P., Zielenska M., (2004), "Defining a 0.5-mb region of genomic gain on chromosome 6p22 in bladder cancer by quantitative-multiplex polymerase chain reaction", *Am J Pathol*, 164, 285-293.

Fairfax K.A., Kallies A., Nutt S.L., Tarlinton D.M., (2008) "Plasma cell development: from B-cell subsets to long-term survival niches", *Semin Immunol*, 20, 49-58.

Falco P., Bringhen S., Avonto I., Gay F., Morabito F., Boccadoro M., Palumbo A., (2007), "Melphalan and its role in the management of patients with multiple myeloma", *Expert Rev Anticancer Ther*, 7, 945-957.

Fonseca R., Bergsagel P.L., Drach J., Shaughnessy J., Gutierrez N., Stewart A.K., Morgan G., Van Ness B., Chesi M., Minvielle S., (2009), "International Myeloma Working Group molecular classification of multiple myeloma: spotlight review", *Leukemia*, 23, 2210-2221.

Fulda S., Debatin K.M., (2006), "Extrinsic versus intrinsic apoptosis pathways in anticancer chemotherapy", *Oncogene*, 25, 4798-4811.

Galson D.L., Silbermann R., Roodman G.D., (2012), "Mechanisms of multiple myeloma bone disease", *Bonekey Rep*, 1, 135.

Gonzalez D., van der Burg M., Garcia-Sanz R., Fenton J.A., Langerak A.W., Gonzalez M., van Dongen J.J., San Miguel J.F., Morgan G.J., (2007), "Immunoglobulin gene rearrangements and the pathogenesis of multiple myeloma", *Blood*, 110, 3112-3121.

Goossens T., Klein U., Kuppers R., (1998), "Frequent occurrence of deletions and duplications during somatic hypermutation: implications for oncogene translocations and heavy chain disease", *Proc Natl Acad Sci*, 95, 2463-2468.

Grasemann C., Gratiass S., Stephan H., Schuler A., Schramm A., Klein-Hitpass L., Rieder H., Schneider S., Kappes F., Eggert A., (2005), "Gains and overexpression identify DEK and E2F3 as targets of chromosome 6p gains in retinoblastoma", *Oncogene*, 24, 6441-6449.

Herzog S., Reth M., Jumaa H., (2009), "Regulation of B-cell proliferation and differentiation by pre-B-cell receptor signalling", *Nature reviews Immunology*, 9, 195-205.

Iwasaki H., Akashi K., (2007), "Hematopoietic developmental pathways: on cellular basis", *Oncogene*, 26, 6687-6696.

Kappes F., Burger K., Baack M., Fackelmayer F.O., Gruss C., (2001), "Subcellular localization of the human proto-oncogene protein DEK", *The Journal of Biological Chemistry*, 276, 26317-26323.

Kappes F., Damoc C., Knippers R., Przybylski M., Pinna L.A., Gruss C., (2004), "Phosphorylation by protein kinase CK2 changes the DNA binding properties of the human chromatin protein DEK", *Mol Cell Biol*, 24, 6011-6020.

Khodadoust M.S., Verhaegen M., Kappes F., Riveiro-Falkenbach E., Cigudosa J.C., Kim D.S., Chinnaiyan A.M., Markovitz D.M., Soengas M.S., (2009), "Melanoma proliferation and chemoresistance controlled by the DEK oncogene", *Cancer Res*, 69, 6405-6413.

Klein U., Dalla-Favera R., (2008), "Germinal centres: role in B-cell physiology and malignancy", *Nat Rev Immunol*, 8, 22-33.

Kondoh N., Wakatsuki T., Ryo A., Hada A., Aihara T., Horiuchi S., Goseki N., Matsubara O., Takenaka K., Shichita M., (1999), "Identification and characterization of genes associated with human hepatocellular carcinogenesis", *Cancer Res*, 59, 4990-4996.

Korbet S.M., Schwartz M.M., (2006), "Multiple myeloma", *J Am Soc Nephrol*, 17, 2533-2545.

Kuehl W.M., Bergsagel P.L., (2002), "Multiple myeloma: evolving genetic events and host interactions", *Nat Rev Cancer*, 2, 175-187.

Kumar S.K., Rajkumar S.V., Dispenzieri A., Lacy M.Q., Hayman S.R., Buadi F.K., Zeldenrust S.R., Dingli D., Russell S.J., Lust J.A., (2008), "Improved survival in multiple myeloma and the impact of novel therapies", *Blood*, 111, 2516-2520.

Kumar S.K., Rajkumar V., Kyle R.A., van Duin M., Sonneveld P., Mateos M.V., Gay F., Anderson K.C., (2017), "Multiple myeloma", *Nat Rev Dis Primers*, 3, 17046.

Kyle R.A., Gertz M.A., Witzig T.E., Lust J.A., Lacy M.Q., Dispenzieri A., Fonseca R., Rajkumar S.V., Offord J.R., Larson D.R., (2003), "Review of 1027 patients with newly diagnosed multiple myeloma", *Mayo Clin Proc*, 78, 21-33.

Lee A.H., Iwakoshi N.N., Glimcher L.H., (2003), "XBP-1 regulates a subset of endoplasmic reticulum resident chaperone genes in the unfolded protein response", *Mol Cell Biol*, 23, 7448-7459.

Logan G.E., Mor-Vaknin N., Braunschweig T., Jost E., Schmidt P.V., Markovitz D.M., Mills K.I., Kappes F., Percy M.J., (2015), "DEK oncogene expression during normal hematopoiesis and in Acute Myeloid Leukemia (AML)", *Blood Cells Mol Dis*, 54, 123-131.

Mahindra A., Hideshima T., Anderson K.C., (2010), "Multiple myeloma: biology of the disease", *Blood Rev*, 24 Suppl 1, S5-11.

Maity P.C., Datta M., Nicolo A., Jumaa H., (2018), "Isotype specific assembly of B cell antigen receptors and synergism with chemokine receptor CXCR4", *Front Immunol*, 9, 2988.

Mor-Vaknin N., Punturieri A., Sitwala K., Faulkner N., Legendre M., Khodadoust M.S., Kappes F., Ruth J.H., Koch A., Glass D., (2006), "The DEK nuclear autoantigen is a secreted chemotactic factor", *Mol Cell Biol*, 26, 9484-9496.

Nemeth M.J., Bodine D.M., (2007), "Regulation of hematopoiesis and the hematopoietic stem cell niche by Wnt signaling pathways", *Cell Res*, 17, 746-758.

Noll J.E., Williams S.A., Tong C.M., Wang H., Quach J.M., Purton L.E., Pilkington K., To L.B., Evdokiou A., Gronthos S., (2014), "Myeloma plasma cells alter the bone marrow microenvironment by stimulating the proliferation of mesenchymal stromal cells", *Haematologica*, 99, 163-171.

Oancea C., Ruster B., Henschler R., Puccetti E., Ruthardt M., (2010), "The t(6;9) associated DEK/CAN fusion protein targets a population of long-term repopulating hematopoietic stem cells for leukemogenic transformation", *Leukemia*, 24, 1910-1919.

Pichiorri F., Suh S.S., Rocci A., De Luca L., Taccioli C., Santhanam R., Zhou W., Benson D.M., Jr., Hofmainster C., Alder H., (2010), "Downregulation of p53-inducible microRNAs 192, 194, and 215 impairs the p53/MDM2 autoregulatory loop in multiple myeloma development", *Cancer Cell*, 18, 367-381.

Pieper K., Grimbacher B., Eibel H., (2013), "B-cell biology and development", *J Allergy Clin Immunol*, 131, 959-971.

Privette Vinnedge L.M., McClaine R., Wagh P.K., Wikenheiser-Brokamp K.A., Waltz S.E., Wells S.I., (2011), "The human DEK oncogene stimulates beta-catenin signaling, invasion and mammosphere formation in breast cancer", *Oncogene*, 30, 2741-2752.

Raab M.S., Podar K., Breitkreutz I., Richardson P.G., Anderson K.C., (2009), "Multiple myeloma", *Lancet*, 374, 324-339.

Rajkumar, S. V. (2014), "International Myeloma Working Group updated criteria for the diagnosis of multiple myeloma", *Lancet Oncol*, 15, e538–e548.

Reagan M.R., Rosen C.J., (2016), "Navigating the bone marrow niche: translational insights and cancer-driven dysfunction", *Nat Rev Rheumatol*, 12, 154-168.

Rieger M.A., Schroeder T., (2012), "Hematopoiesis", *Cold Spring Harb Perspect Biol*, 4.

Riveiro-Falkenbach E., Soengas M.S., (2010), "Control of tumorigenesis and chemoresistance by the DEK oncogene", *Clin Cancer Res*, 16, 2932-2938.

Saha A.K., Kappes F., Mundade A., Deutzmann A., Rosmarin D.M., Legendre M., Chatain N., Al-Obaidi Z., Adams B.S., Ploegh H.L., (2013), "Intercellular trafficking of the nuclear oncoprotein DEK", *Proc Natl Acad Sci*, 110, 6847-6852.

Scarcello E., Lambremont A., Vanbever R., Jacques P.J., Lison D., (2020), "Mind your assays: Misleading cytotoxicity with the WST-1 assay in the presence of manganese", *PLoS One*, 15, e0231634.

Schlissel M.S., (2003), "Regulating antigen-receptor gene assembly", *Nat Rev Immunol*, 3, 890-899.

Seita J., Weissman I.L., (2010), "Hematopoietic stem cell: self-renewal versus differentiation", *Wiley Interdisciplinary Reviews Systems Biology and Medicine*, 2, 640-653.

Shaffer A.L., Lin K.I., Kuo T.C., Yu X., Hurt E.M., Rosenwald A., Giltnane J.M., Yang L., Zhao H., Calame K., (2002), "Blimp-1 orchestrates plasma cell differentiation by extinguishing the mature B cell gene expression program", *Immunity*, 17, 51-62.

Shapiro-Shelef M., Calame K., (2005), "Regulation of plasma-cell development", *Nature Reviews Immunology*, 5, 230-242.

Singhal S., Mehta J., (2006), "Multiple myeloma", *Clin J Am Soc Nephrol*, 1, 1322-1330.

Sirohi B., Powles R., (2004), "Multiple myeloma", *Lancet*, 363, 875-887.

Slovak M.L., (2011), "Multiple myeloma: current perspectives", *Clin Lab Med*, 31, 699-724, x.

Smith C., (2003), "Hematopoietic stem cells and hematopoiesis", *Cancer Control: Journal of the Moffitt Cancer Center*, 10, 9-16.

Smith E.A., Kumar B., Komurov K., Smith S.M., Brown N.V., Zhao S., Kuma, P., Teknos T.N., Wells S.I., (2017), "DEK associates with tumor stage and outcome in HPV16 positive oropharyngeal squamous cell carcinoma", *Oncotarget*, 8, 23414-23426.

Solary E., Guiguet M., Zeller V., Casasnovas R.O., Caillot D., Chavanet P., Guy H., Mack G., (1992), "Radioimmunoassay for the measurement of serum IL-6 and its correlation with tumour cell mass parameters in multiple myeloma", *Am J Hematol*, 39, 163-171.

Stephens O.W., Zhang Q., Qu P., Zhou Y., Chavan S., Tian E., Williams D.R., Epstein J., Barlogie B., Shaughnessy J.D., Jr., (2012), "An intermediate-risk multiple myeloma subgroup is defined by sIL-6r: levels synergistically increase with incidence of SNP rs2228145 and 1q21 amplification", *Blood*, 119, 503-512.

Tabbert A., Kappes F., Knippers R., Kellermann J., Lottspeich F., Ferrando-May E., (2006), "Hypophosphorylation of the architectural chromatin protein DEK in death-receptor-induced apoptosis revealed by the isotope coded protein label proteomic platform", *Proteomics*, 6, 5758-5772.

Tokoyoda K., Egawa T., Sugiyama T., Choi B.I., Nagasawa T., (2004), "Cellular niches controlling B lymphocyte behavior within bone marrow during development", *Immunity*, 20, 707-718.

Tsai D.Y., Hung K.H., Chang C.W., Lin K.I., (2019), "Regulatory mechanisms of B cell responses and the implication in B cell-related diseases", *J Biomed Sci*, 26, 64.

Turner C.A., Jr., Mack D.H., Davis M.M., (1994), "Blimp-1, a novel zinc finger-containing protein that can drive the maturation of B lymphocytes into immunoglobulin-secreting cells", *Cell*, 77, 297-306.

von Lindern M., Fornerod M., van Baal S., Jaegle M., de Wit T., Buijs A., Grosveld G., (1992), "The translocation (6;9), associated with a specific subtype of acute myeloid leukemia, results in the fusion of two genes, *dek* and *can*, and the expression of a chimeric, leukemia-specific *dek-can* mRNA", *Mol Cell Biol*, 12, 1687-1697.

Waldmann T., Scholten I., Kappes F., Hu H.G., Knippers R., (2004), "The DEK protein--an abundant and ubiquitous constituent of mammalian chromatin", *Gene*, 343, 1-9.

Walker B.A., Leone P.E., Chiecchio L., Dickens N.J., Jenner M.W., Boyd K.D., Johnson D.C., Gonzalez D., Dagrada G.P., Protheroe R.K., (2010), "A compendium of myeloma-associated chromosomal copy number abnormalities and their prognostic value", *Blood*, 116, e56-65.

Web 1, (2022), <https://www.atcc.org/products/crl-2496>, (Access Date: 18/09/22).

Web 2, (2022), <https://www.atcc.org/products/crl-11882>, (Access Date: 18/09/22).

Web 3, (2022), <https://www.atcc.org/products/tib-196>, (Access Date: 18/09/22).

Web 4, (2022), <https://www.atcc.org/products/crm-ccl-155>, (Access Date: 18/09/22).

Web 5, (2022), <https://www.addgene.org/27490/>, (Access Date: 18/09/22).

Web 6, (2022), <http://www.biorad.com/webroot/web/pdf/lsr/literature/10020688.pdf>, (Access Date: 17/09/22).

Wise-Draper T.M., Allen H.V., Jones E.E., Habash K.B., Matsuo H., Wells S.I., (2006), "Apoptosis inhibition by the human DEK oncoprotein involves interference with p53 functions", *Mol Cell Biol*, 26, 7506-7519.

Wise-Draper T.M., Morreale R.J., Morris T.A., Mintz-Cole R.A., Hoskins E.E., Balsitis S.J., Husseinzadeh N., Witte D.P., Wikenheiser-Brokamp K.A., Lambert P.F., (2009), "DEK proto-oncogene expression interferes with the normal epithelial differentiation program", *Am J Pathol*, 174, 71-81.

Yang B., Yu R.L., Chi X.H., Lu X.C., (2013), "Lenalidomide treatment for multiple myeloma: systematic review and meta-analysis of randomized controlled trials", *PloS One*, 8, e64354.

Young C., Lau A.W.Y., Burnett D.L., (2022), "B cells in the balance: Offsetting self-reactivity avoidance with protection against foreign", *Front Immunol*, 13, 951385.

Yu L., Huang X., Zhang W., Zhao H., Wu G., Lv F., Shi L., Teng Y., (2016), "Critical role of DEK and its regulation in tumorigenesis and metastasis of hepatocellular carcinoma", *Oncotarget*, 7, 26844-26855.

Zhao E., Xu H., Wang L., Kryczek I., Wu K., Hu Y., Wang G., Zou W., (2012), "Bone marrow and the control of immunity", *Cell Mol Immunol*, 9, 11-19.



BIOGRAPHY

Türkan Güzel completed her undergraduate education at Izmir Institute of Technology, Department of Molecular Biology and Genetics, between 2006-2011. In 2014, she finished her master's degree at Gebze Technical University (former name Gebze Institute of Technology), Department of Molecular Biology and Genetics. She started her PhD studies in 2014 in the same department. Türkan Güzel worked as a research assistant in the same department from 2012 to 2021.



APPENDICES

Appendix A: The Paper Published within the Scope of the Thesis

Cakar T., Kandilci A., (2019), “Analysis of the effect of DEK overexpression on the survival and proliferation of bone marrow stromal cells”, Turkish Journal of Biochemistry, 44(4).

Cakar T., Kandilci A., (2020), “DEK promotes expression of IL-6 in the human bone marrow stromal cells” 25th Congress of the European Hematology Association Virtual Edition 2020, HemaSphere, 2020; 4: S1, Page 1049. (Poster)

